J. Fluid Mech. (2022), *vol*. 945, A1, doi:10.1017/jfm.2022.481

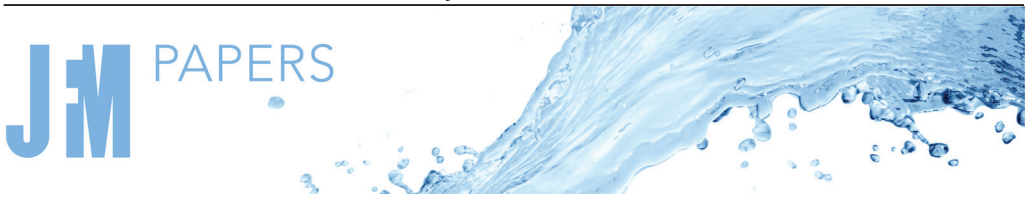

Anisotropic stresslet and rheology of stick–slip Janus spheres

A.R. Premlata[1] **and Hsien-Hung Wei**[1],†

[1]Department of Chemical Engineering, National Cheng Kung University, Tainan 701, Taiwan

(Received 9 February 2022; revised 10 May 2022; accepted 24 May 2022)

A Janus sphere with a stick–slip pattern can behave quite differently in its hydrodynamics compared with a no-slip or uniform-slip sphere. Here, using the Lorentz reciprocal theorem in conjunction with surface harmonic expansion, we rigorously derive the extended Faxén formula for the stresslet of a weakly stick–slip Janus sphere, capable of describing the anisotropic nature of the stresslet with an arbitrary axisymmetric stick–slip pattern in an arbitrary background flow. We find that slip anisotropy not only causes a variety of additional contributions to the stresslet, but also naturally renders a stresslet–rotation coupling that may turn a suspension of couple-free stick–slip Janus spheres into a dipolar one under the actions of an external couple. Moreover, to correctly account for the impacts of slip anisotropy on the stresslet, it is necessary to include at least the first four surface harmonic contributions. As a result, the anisotropies of both the stresslet and torque on the sphere in a linear flow field are purely reflected by a symmetric quadrupole and hexadecapole. These hydrodynamic quantities can be further mediated by an antisymmetric dipole and octupole due to the gradients of the imposed strain field. The average bulk stress and effective viscosity for a suspension of stick–slip spheres are also determined, showing characteristics quite distinct from those of a suspension of near spheres. If the spheres possess permanent dipole moments, in particular, additional stresslets and couplets can be generated by an applied external couple on each sphere and added into the bulk stress, accompanied by non-Jeffery orientational orbits of such dipolar stick–slip spheres. In addition to the above, the extended Faxén stresslet and torque relations found in this work will also provide the formulae needed for tackling problems involving hydrodynamically interacting stick–slip spheres on which small slip anisotropy may have profound impacts.

Key words: low-Reynolds-number flows

† Email address for correspondence: hhwei@mail.ncku.edu.tw

1. Introduction

In the study of particle motion under low-Reynolds-number conditions, apart from the need for finding the hydrodynamic force and torque on a single particle, it is often of interest to determine the bulk viscosity of a particle suspension due to the excess stress imparted by suspended particles. The stresslet is the key quantity that measures the additional dissipation by the particles in the ambient fluid.

A stresslet is a symmetric force dipole, defined by the following integral over the surface (S_p) of a particle (Batchelor 1970):

$$\mathcal{S}_{ij} = \frac{1}{2}\int_{S_p}\left[(x_j\sigma_{ik}n_k + x_i\sigma_{jk}n_k) - \frac{2}{3}\delta_{ij}x_l\sigma_{lk}n_k - 2\mu(u_jx_i + u_ix_j)\right]\mathrm{d}S, \tag{1.1}$$

where u_i and σ_{ij} stand, respectively, for the fluid velocity and stress at position x_i, with the origin chosen at the particle's centre and n_i being the unit surface normal pointing into the fluid. The surface velocity term comes from the double layer contribution in the integral representation of the Stokes flow solution (Kim & Karrila 1991), and can contribute to a stresslet if a particle is not rigid or the no-slip boundary condition is not satisfied. For a no-slip spherical particle of radius a, the stresslet is (Batchelor & Green 1972*b*)

$$\mathcal{S}_{ij} = \frac{20\pi}{3}\mu a^3 E_{ij}, \tag{1.2}$$

where E_{ij} is the rate of strain tensor. With the average particle stress $\phi\mathcal{S}_{ij}/(4\pi a^3/3)$, the effective viscosity can be found in terms of particle volume fraction ϕ:

$$\mu_{eff} = \mu(1 + 2.5\phi), \tag{1.3}$$

which is the well known Einstein relation (Einstein 1906; Batchelor & Green 1972*b*; Landau & Lifshitz 1987). For slip particles such as in aerosols and hydrophobic colloids, the stresslet is further affected by the slip length $a\hat{\lambda}$ (Keh & Chen 1996; Luo & Pozrikidis 2008):

$$\mathcal{S}_{ij} = \frac{20}{3}\left(\frac{1 + 2\hat{\lambda}}{1 + 5\hat{\lambda}}\right)\pi\mu a^3 E_{ij}. \tag{1.4}$$

It is evident that the stresslet in this case will be less than (1.2) because of less viscous stress on the slippery surface of the particle. For a drop, the stresslet is characterized by the viscosity ratio κ of the drop to the bulk fluid (Rallison 1978):

$$\mathcal{S}_{ij} = \frac{4}{3}\left(\frac{5\kappa + 2}{\kappa + 1}\right)\pi\mu a^3 E_{ij}. \tag{1.5}$$

In fact, the inverse of this viscosity ratio can be used to measure the amount of slip: $\kappa = 1/(5\hat{\lambda})$. A similar analogy can also occur between the drag on a slip particle and that on a viscous drop (Premlata & Wei 2019).

In the present work, we examine how slip anisotropy modifies the features of the stresslet on a non-uniform slip particle. Our work is motivated by the need for understanding

the hydrodynamics of a stick–slip Janus particle which has a dipolar-like surface made of hydrophilic and hydrophobic portions (Jiang *et al.* 2008). The stresslet on such heterogeneous particle will play a crucial role in determining the corresponding suspension rheology. Our work is also closely relevant to the swimming of a squirmer self-propelled by a prescribed tangential velocity over its surface (Lighthill 1952; Blake 1971; Wang & Ardekani 2012; Pedley 2016). To maximize the propulsion, a squirmer can be made of both stick-hydrophilic and slip-hydrophobic portions such that the driving squirming actions are executed only on the stick surface, while the slip surface serves to reduce the drag force on the squirmer. How much power is required for the squirmer to propel itself will be determined by the stresslet on it.

The stresslet of a non-uniform slip sphere can differ fundamentally from that of a uniform-slip sphere. In the latter, the stresslet is commonly determined by the rate of strain tensor as given by (1.4). However, if placing a stick–slip–stick Janus sphere at the centre of a purely straining flow, for instance, it can spin due to the antisymmetric force pair acting on the stick caps (Premlata & Wei 2021). This implies that an additional stresslet may arise from a couple on such a striped Janus sphere when it is placed in a purely rotating flow. In this case, because the force couples on the stick portion and the slip portion are unequal, the sphere will still feel a non-zero symmetric force moment, namely a stresslet, due to these asymmetric force couples, contrary to the uniform-slip counterpart where no stresslet can be produced in the same flow environment. In other words, both straining and vorticity components of a linear flow field can contribute to the stresslet on a non-uniform slip sphere, whereas only the straining component is responsible for the stresslet on a uniform-slip sphere. This follows therefore that for a non-uniform slip sphere, its stresslet from the symmetrical part of a force dipole may no longer be unaffected by the couple from the antisymmetric part of a force dipole. In fact, it has been shown by Batchelor (1970) that based on symmetry considerations, a stresslet generally consists of an additional contribution from a couple. As also pointed out by Batchelor, whether the determination of stresslet can be separated from that of a couple lies in whether symmetry properties of a particle can be preserved, depending on its shape and orientation. The stick–slip asymmetry of a non-uniform slip sphere basically affects both the shape (because of the varying hydrodynamic drag coefficient) and orientation (because of the stick–slip director) of the sphere. For this reason, for a non-uniform slip sphere, even though its stick–slip pattern is axisymmetric, it may not necessarily behave like a spheroid but more like an asymmetric doublet. Consequently, the features of the stresslet for a stick–slip Janus sphere may not resemble those for a spheroid.

Another motivation of the present work is to clarify the results in early studies by Khair and his coworkers. Swan & Khair (2008) derived the Faxén relations for a weakly stick–slip Janus sphere. Their results were written in the integral form obtained by taking multipole moment expansions of the singularity solutions of Stokes flow. They found that either the imposed strain field or the sphere's angular velocity can be expressed in terms of both the stresslet and torque on the sphere in a given flow field. This indicates that stresslet–rotation coupling and torque-strain coupling can exist in the motion of the sphere. However, it is not clear how both the stresslet and torque are determined by the stick–slip pattern of the sphere. In particular, if the surface of the sphere is not equally partitioned by stick and slip parts, it will actually comprise both surface dipole and quadrupole contributions (Premlata & Wei 2021). We recently showed that these surface moments can have rather distinct impacts on the force and torque on a non-uniform slip sphere (Premlata & Wei 2021). This raises a question: How do distinct surface

moments determine the anisotropic nature of the stresslet on a non-uniform slip sphere? Especially, which surface moment will be responsible for the stresslet–rotation coupling found by Swan & Khair (2008)? It has been shown that the force–rotation coupling due to slip anisotropy, which was also found by Swan & Khair (2008), is responsible by a surface dipole (Premlata & Wei 2021). These different couplings are likely triggered by different surface moments corresponding to distinct stick–slip symmetries/asymmetries, implying that such couplings may not always coexist, depending on the surface pattern of a non-uniform slip sphere.

In the subsequent study by Ramachandran & Khair (2009), they analysed the motion of a two-faced stick–slip sphere in a linear flow field and solved the detailed flow field around the sphere in terms of Lamb's solution. In determining the motion of the sphere, they made the sphere analogous to a doublet (Nir & Acrivos 1973) or a spheroid (Kim & Karrila 1991) and used linearity arguments to construct the expressions for the translational and angular velocities with the coefficients determined from the flow solution they obtained. However, such an analogy may depend on the surface pattern of a Janus sphere. If the sphere is precisely half-faced, the surface pattern is antisymmetric, represented by a surface dipole (Premlata & Wei 2021). While an analogy to a doublet can be made by letting the two touched spheres be of different sizes, no correspondence to a two-faced Janus sphere can be found if the doublet becomes perfectly symmetric by letting the two spheres be of equal size. In fact, a symmetric doublet or spheroid may be a better analogous model for a stick–slip–stick/slip–stick–slip Janus of striped type whose surface pattern is symmetric represented by a surface quadrupole (Premlata & Wei 2021). Because the two Janus sphere types mentioned above represent distinct symmetries in geometry, the corresponding stresslets should behave differently. Ramachandran & Khair (2009) adopted a general expression from Ericksen (1959) to determine the stresslet of a stick–slip Janus sphere, similar to the approach of determining the stresslet of a doublet or a spheroid (Nir & Acrivos 1973). The expression involves a variety of polyadic contributions of the stick–slip director. However, it is not clear how these contributions are determined by distinct symmetric and antisymmetric surface moments that constitute the surface of the sphere. Also given that the complete description of a stresslet further involves a couple (due to external torque) (Batchelor 1970), the stresslet expression adopted by Ramachandran & Khair (2009) may also need to be revised to include this additional contribution. Including a couple to the stresslet expression is also necessary in order to be conceptually consistent with the stresslet–rotation coupling found by Swan & Khair (2008).

As such, all these issues mentioned above will not only be essential to understanding the anisotropic nature of a stick–slip sphere, but also critical to the rheology of a suspension made of such heterogeneous spheres. These issues will be better addressed with a more general approach enabling us to systemically decode how the stresslet is determined by the stick–slip asymmetry without having to solve the detailed flow field around the sphere, which is the main theme of this work.

Our paper is organized as follows. In § 2, we first develop a general formulation needed for computing the stresslet of a weakly stick–slip sphere. With the aid of surface moments to re-express impacts of slip anisotropy in § 3, we use this general formulation to derive the Faxén relation for the stresslet as well as that for the torque in § 4. Subsequent impacts on the rheology of a suspension of stick–slip spheres and their orientational dynamics with and without an external couple will be presented in §§ 5 and 6. We conclude this work along with relevant perspectives in § 7.

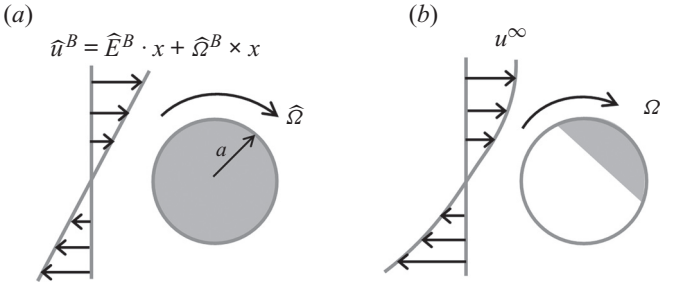

Figure 1. The selected problems for applying the reciprocal theorem. (*a*) The auxiliary problem: a uniform-slip sphere (of radius a and slip length $a\hat{\lambda}$) in a linear flow field $\hat{u}_i^B$. The sphere is located at the zero velocity plane of the flow. It does not translate with the flow, but can rotate at an angular velocity $\hat{\Omega}_i$. (*b*) The problem of interest: a stick–slip sphere in an arbitrary background flow field u_i^∞. The sphere is positioned at the zero velocity plane of the flow without translation, but allowed to rotate at an angular velocity Ω_i. Here the slip surface is schematized by grey, in contrast to white for the stick (no-slip) surface.

2. Formulation: stresslet–rotation coupling for a non-uniform slip sphere

A stick–slip sphere at the centre of a purely straining flow may spin (Premlata & Wei 2021) to cause an additional stresslet to the sphere. So the stresslet on the sphere will be determined not only by the strain rate of a flow but also by the rotation of the sphere. Such stresslet–rotation coupling is a generic feature of a non-uniform slip sphere and has to be part of the description of its stresslet, in contrast to a no-slip or uniform-slip sphere whose stresslet is determined solely by the strain rate of a flow.

To establish the formula for computing the stresslet of a non-uniform slip sphere, we begin with the Lorentz reciprocal theorem (Happel & Brenner 1983):

$$\int_{S_p} \hat{u}_i' \sigma_{ik}' n_k \,\mathrm{d}S = \int_{S_p} u_i' \hat{\sigma}_{ik}' n_k \,\mathrm{d}S. \tag{2.1}$$

Here $(\hat{u}', \hat{\sigma}')$ and (u', σ') are two different solutions of disturbance velocity and stress fields satisfying the Stokes flow equations $\boldsymbol{\nabla} \cdot \hat{u}' = \boldsymbol{\nabla} \cdot u' = 0$ and $\boldsymbol{\nabla} \cdot \hat{\sigma}' = \boldsymbol{\nabla} \cdot \sigma' = 0$. These disturbance velocity and stress fields decay, respectively, as $1/r$ and $1/r^2$ (or faster) as distance r to the sphere becomes large. As illustrated in figure 1, we select $(\hat{u}', \hat{\sigma}')$ to be the solution to the auxiliary problem (figure 1*a*) for a uniform-slip sphere (of radius a and slip length $a\hat{\lambda}$) in a linear flow field with the velocity and stress fields

$$\hat{u}_i^B = \hat{E}_{ij}^B x_j + \epsilon_{ijk} \hat{\Omega}_j^B x_k, \tag{2.2a}$$

$$\hat{\sigma}_{ij}^B = 2\mu \hat{E}_{ij}^B, \tag{2.2b}$$

where $\hat{E}_{ij}^B$ and $\hat{\Omega}_j^B = (1/2)\epsilon_{jpq} \partial \hat{u}_q^B / \partial x_p$ are the straining and vorticity components, respectively, and μ is the viscosity of the fluid. For simplicity, we assume that the sphere is located at the zero velocity plane of the flow so that it does not translate with the flow but can rotate at an angular velocity $\hat{\Omega}_i$.

For the problem we wish to solve for a non-uniform slip sphere (figure 1*b*), (u', σ') is yet to be determined. The sphere has a spatially varying slip length $a\lambda(\boldsymbol{x})$ and is immersed in an arbitrary background flow field u_i^∞ which can be nonlinear. The background stress field is σ_{ik}^∞. Again, we assume that the sphere is positioned at the zero velocity plane of the flow without translation, but allowed to rotate at an angular velocity Ω_i.

With the set-up above, the actual velocity and stress fields in a fixed frame are

$$(\hat{u}_i, \hat{\sigma}_{ij}) = (\hat{u}'_i, \hat{\sigma}'_{ij}) + (\hat{u}^B_i, \hat{\sigma}^B_{ij}), \quad (u_i, \sigma_{ij}) = (u'_i, \sigma'_{ij}) + (u^\infty_i, \sigma^\infty_{ij}). \tag{2.3a,b}$$

In the former for the auxiliary problem, the force density $\hat{\sigma}_{ij}n_j$ on the surface of the uniform-slip sphere can be expressed in terms of the known strain resistance tensor Σ_{ilk} and rotation resistance tensor R_{ip} :

$$\hat{\sigma}_{ij}n_j = \mu\Sigma_{ilk}\hat{E}^B_{lk} + \mu R_{ip}\epsilon_{pqs}(\hat{\Omega}^B_q - \hat{\Omega}_q)x_s. \tag{2.4}$$

The two problems are subject to similar sets of boundary conditions on the respective sphere's surfaces as follows. For the auxiliary problem, the uniform-slip sphere is constrained by the no-penetration condition and the slip boundary condition on its surface:

$$(\hat{u}'_i - \epsilon_{ikl}\hat{\Omega}_k x_l + \hat{u}^B_i)n_i = 0, \tag{2.5a}$$

$$(\hat{u}'_j - \epsilon_{jkl}\hat{\Omega}_k x_l + \hat{u}^B_j)(\delta_{ij} - n_i n_j) = \frac{a\hat{\lambda}}{\mu}\hat{\sigma}_{jm}n_m(\delta_{ij} - n_i n_j). \tag{2.5b}$$

Similarly, for the problem we wish to solve for a non-uniform slip sphere, the boundary conditions on the sphere's surface are

$$(u'_i - \epsilon_{ikl}\Omega_k x_l + u^\infty_i)n_i = 0, \tag{2.6a}$$

$$(u'_j - \epsilon_{jkl}\Omega_k x_l + u^\infty_j)(\delta_{ij} - n_i n_j) = \frac{a\lambda(\boldsymbol{x})}{\mu}\sigma_{jm}n_m(\delta_{ij} - n_i n_j). \tag{2.6b}$$

To form a stresslet according to (1.1), we incorporate $\hat{u}^B_i$ given by (2.2*a*) into the left-hand side of (2.1) to separate the straining part and rotational part. With these, we rewrite the left-hand side of (2.1) as

$$\begin{aligned}\int_{S_p} \hat{u}'_i\sigma'_{ik}n_k \,\mathrm{d}S = -\hat{E}^B_{ij}\int_{S_p} x_j\sigma'_{ik}\, n_k \,\mathrm{d}S - (\hat{\Omega}^B_j - \hat{\Omega}_j)\int_{S_p} \epsilon_{jmi}\, x_m\, \sigma'_{ik}\, n_k \,\mathrm{d}S \\ + \int_{S_p} (\hat{u}'_i - \epsilon_{ikm}\hat{\Omega}_k x_m + \hat{u}^B_i)\sigma'_{ij}n_j \,\mathrm{d}S.\end{aligned} \tag{2.7}$$

The second term on the right-hand side gives the hydrodynamic torque on the sphere:

$$\mathcal{L}_j = \int_{S_p} \epsilon_{jmi}x_m\sigma'_{ik}n_k \,\mathrm{d}S. \tag{2.8}$$

In the last term of (2.7), we recognize that the surface velocity only acts tangentially along the sphere surface in view of (2.5*a*). This allows us to replace the surface velocity by the slip term using (2.5*b*). Further writing $\sigma'_{ik} = \sigma_{ik} - \sigma^\infty_{ik}$, the last term of (2.7) can be

re-expressed as

$$\int_{S_p}(\hat{u}_i' - \epsilon_{ikm}\hat{\Omega}_k x_m + \hat{u}_i^B)\sigma_{ij}' n_j \,\mathrm{d}S = \frac{a}{\mu}\int_{S_p}\hat{\lambda}\,\hat{\sigma}_{jm}\,n_m\,(\delta_{ij}-n_i n_j)\sigma_{ik}n_k\,\mathrm{d}S - \frac{a}{\mu}\int_{S_p}\hat{\lambda}\hat{\sigma}_{jm}n_m(\delta_{ij}-n_i n_j)\sigma_{ik}^{\infty}n_k\,\mathrm{d}S. \tag{2.9}$$

As for the right-hand side of (2.1), we use $\hat{\sigma}_{ik}' = \hat{\sigma}_{ik} - \hat{\sigma}_{ik}^B$ and (2.2*b*) to extract the velocity part for the stresslet:

$$\int_{S_p} u_i'\hat{\sigma}_{ik}' n_k \,\mathrm{d}S = -2\mu\hat{E}_{ik}^B\int_{S_p}u_i' n_k\,\mathrm{d}S + \int_{S_p}u_i'\hat{\sigma}_{ik}n_k\,\mathrm{d}S. \tag{2.10}$$

The last term in (2.10) can be rewritten as

$$\int_{S_p} u_i'\hat{\sigma}_{ik}n_k\,\mathrm{d}S = \int_{S_p}(u_i' - \epsilon_{ijm}\Omega_j x_m + u_i^{\infty})\hat{\sigma}_{ik}n_k\,\mathrm{d}S + \Omega_j\int_{S_p}\epsilon_{jmi}x_m\hat{\sigma}_{ik}n_k\,\mathrm{d}S - \int_{S_p}u_i^{\infty}\hat{\sigma}_{ik}n_k\,\mathrm{d}S. \tag{2.11}$$

Again, the second term on the right-hand side provides the hydrodynamic torque on the uniform-slip sphere:

$$\hat{\mathcal{L}}_j = \int_{S_p}\epsilon_{jmi}x_m\hat{\sigma}_{ik}n_k\,\mathrm{d}S. \tag{2.12}$$

Note that this torque can be non-zero if there is an external couple applied to the sphere which will spin at $\hat{\Omega}_j \neq \hat{\Omega}_j^B$. The velocity part in the first term on the right-hand side of (2.11) can be replaced by the slip term with the aid of (2.6*a*) and (2.6*b*):

$$\int_{S_p}(u_i' - \epsilon_{ijm}\Omega_j x_m + u_i^{\infty})\hat{\sigma}_{ik}n_k\,\mathrm{d}S = \frac{\mu}{a}\int_{S_p}\lambda(\boldsymbol{x})\sigma_{jm}n_m(\delta_{ij}-n_i n_j)\hat{\sigma}_{ik}n_k\,\mathrm{d}S. \tag{2.13}$$

Combining (2.7)–(2.13), we obtain the following joint expression for the stresslet $\mathcal{S}_{ij}$ and torque $\mathcal{L}_k$ on a non-uniform slip sphere, representing its rate of dissipation energy:

$$\hat{E}_{ij}^B\mathcal{S}_{ij} + (\hat{\Omega}_k^B - \hat{\Omega}_k)\mathcal{L}_k = \int_{S_p}u_i^{\infty}\hat{\sigma}_{ij}n_j\,\mathrm{d}S - \Omega_k\hat{\mathcal{L}}_k - \frac{a}{\mu}\int_{S_p}\hat{\lambda}\sigma_{jm}^{\infty}n_m(\delta_{ij}-n_i n_j)\hat{\sigma}_{ik}n_k\,\mathrm{d}S - \frac{a}{\mu}\int_{S_p}(\lambda(\boldsymbol{x})-\hat{\lambda})(\sigma_{jm}'n_m + \sigma_{jm}^{\infty}n_m)(\delta_{ij}-n_i n_j)\hat{\sigma}_{il}n_l\,\mathrm{d}S. \tag{2.14}$$

If the sphere is uniform-slip with $\lambda(\boldsymbol{x}) = \hat{\lambda}$, (2.14) is reduced to

$$\hat{E}_{ij}^B\mathcal{S}_{ij} + (\hat{\Omega}_k^B - \hat{\Omega}_k)\mathcal{L}_k = \int_{S_p}u_i^{\infty}\hat{\sigma}_{ij}n_j\,\mathrm{d}S - \int_{S_p}\hat{u}_i\sigma_{ij}^{\infty}n_j\,\mathrm{d}S - \Omega_k(\hat{\mathcal{L}}_k - \mathcal{L}_k^{\infty}), \tag{2.15}$$

recovering the stresslet formula derived by Keh & Chen (1996) under the couple-free condition $\mathcal{L}_k^{\infty} = \int_{S_p}\epsilon_{kmi}x_m\sigma_{ij}^{\infty}n_j\,\mathrm{d}S = 0$ and $\hat{\mathcal{L}}_k = 8\pi\mu a^3(1+3\hat{\lambda})^{-1}(\hat{\Omega}_k^B - \hat{\Omega}_k) = 0$.

On the other hand, if the slip length varies along the sphere's surface, the last term in (2.14) represents effects of slip anisotropy. Since this term involves the unknown force density $\sigma_{jm}n_m = \sigma'_{jm}n_m + \sigma^{\infty}_{jm}n_m$, we determine both $\mathcal{S}_{ij}$ and $\mathcal{L}_k$ approximately by assuming that the magnitude of the slip variation $|\lambda(\boldsymbol{x}) - \hat{\lambda}|$, ε, is small compared with unity. The average slip length $a\langle\lambda(\boldsymbol{x})\rangle$ is set to be $a\hat{\lambda}$ so that we can formulate the desired non-uniform-slip problem in reference to the auxiliary uniform-slip problem. Note that $\langle\lambda(\boldsymbol{x})\rangle$ can be small, especially in the case of weakly stick–slip spheres whose stick–slip contrasts are small. With $\varepsilon \ll 1$, the unknown disturbance force density $\sigma'_{jm}n_m$ in the slip variation integral can be taken as the uniform-slip contribution plus an $O(\varepsilon)$ slip anisotropy correction:

$$\sigma'_{jm}n_m = \sigma'^{(0)}_{jm}n_m + O(\varepsilon). \tag{2.16}$$

With (2.16), the slip variation integral in (2.14) can be kept accurate to $O(\varepsilon)$, and hence $\mathcal{S}_{ij}$ and $\mathcal{L}_k$. With (2.16) in (2.14), we can establish the approximate formulae for $\mathcal{S}_{ij}$ and $\mathcal{L}_k$ in a more systematic manner as follows.

We first re-express $\sigma'^{(0)}_{jm}n_m$ in terms of the strain resistance tensor $\Sigma'_{jlk} = \Sigma_{jlk} - 2\mu\delta_{jl}n_k$ and the rotation resistance tensor R_{jp} given in (2.4) from the uniform-slip problem,

$$\sigma'^{(0)}_{jm}n_m = \mu\,\Sigma'_{jlk}E^{\infty}_{lk}(0) + \mu R_{jp}\epsilon_{pqs}(\Omega^{\infty}_q(0) - \Omega_q)x_s, \tag{2.17}$$

allowing us to write the force density in a linear form of the strain rate $E^{\infty}_{lk}(0)$ and the rate of rotation $(\Omega^{\infty}_q(0) - \Omega_q)$ at the sphere's centre '0'. Since the imposed flow stress σ^{∞}_{jm} involves $E^{\infty}_{jm}(0)$, it is also necessary to expand σ^{∞}_{jm} in the slip variation term as

$$\sigma^{\infty}_{jm} = -p^{\infty}(0)\delta_{jm} + 2\mu E^{\infty}_{jm}(0) + \Delta^{\infty}_{jm}|_0, \tag{2.18}$$

where $\Delta^{\infty}_{jm}|_0 = x_p\nabla_p\sigma^{\infty}_{jm}|_0 + (x_px_q/2)\nabla_p\nabla_q\sigma^{\infty}_{jm}|_0 + \cdots$. With (2.17) and (2.18), $(\sigma'_{jm}n_m + \sigma^{\infty}_{jm}n_m)$ in the slip variation term in (2.14) can be approximated as

$$\begin{aligned}\sigma'_{jm}n_m + \sigma^{\infty}_{jm}n_m = {}& \mu[\Sigma_{jlk}E^{\infty}_{lk}(0) + R_{jp}\epsilon_{pqs}(\Omega^{\infty}_q(0) - \Omega_q)x_s] \\ & - p^{\infty}(0)\delta_{jm}n_m + \Delta^{\infty}_{jm}|_0 n_m + O(\varepsilon).\end{aligned} \tag{2.19}$$

Using (2.19) in (2.16) and writing $\hat{\sigma}_{jm}n_m$ in terms of the resistance tensors in (2.4), together with $\Sigma^{\parallel}_{jlk} = \Sigma_{ilk}(\delta_{ij} - n_in_j)$ and $R^{\parallel}_{jp} = R_{ip}(\delta_{ij} - n_in_j)$ acting tangentially along the sphere's surface, we can transform (2.14) into the following grand matrix form:

$$\begin{bmatrix}\hat{E}^B_{ij}, & (\hat{\Omega}^B_k - \hat{\Omega}_k)\end{bmatrix}\begin{bmatrix}\mathcal{S}_{ij} \\ \mathcal{L}_k\end{bmatrix} = \begin{bmatrix}\hat{E}^B_{ij}, & (\hat{\Omega}^B_k - \hat{\Omega}_k)\end{bmatrix}\begin{bmatrix}R^E_{ij} \\ R^{\Omega}_k\end{bmatrix}, \tag{2.20}$$

where the tensors R^E_{ij} and R^{Ω}_{k} are given by

$$\begin{aligned} R^E_{ij} &= \mu\int_{S_p}\Sigma_{mij}u^{\infty}_m\,\mathrm{d}S - a\hat{\lambda}\int_{S_p}\Sigma^{\parallel}_{mij}\sigma^{\infty}_{ml}n_l\,\mathrm{d}S \\ &\quad - a\mu\int_{S_p}\varepsilon f(\boldsymbol{x})\,\Sigma^{\parallel}_{mij}\big[\Sigma_{mpq}E^{\infty}_{pq}(0) + R_{mn}\,\epsilon_{nrs}(\Omega^{\infty}_r(0) - \Omega_r)x_s\big]\,\mathrm{d}S \\ &\quad - a\int_{S_p}\varepsilon f(\boldsymbol{x})\,\Sigma^{\parallel}_{mij}(-p^{\infty}(0)n_m + \Delta^{\infty}_{ml}\big|_0\,n_l)\,\mathrm{d}S \\ &\quad - \mu\int_{S_p}\Sigma_{nij}\epsilon_{nrs}(\Omega^{\infty}_r(0) - \Omega_r)x_s\,\mathrm{d}S, \end{aligned} \tag{2.21a}$$

$$\begin{aligned} R^{\Omega}_{k} &= \mu\int_{S_p}\epsilon_{kln}x_l\,R_{mn}u^{\infty}_m\,\mathrm{d}S - a\hat{\lambda}\int_{S_p}\epsilon_{kln}x_lR^{\parallel}_{mn}\sigma^{\infty}_{mj}n_j\,\mathrm{d}S \\ &\quad - a\mu\int_{S_p}\varepsilon f(\boldsymbol{x})\epsilon_{kln}x_l\,R^{\parallel}_{mn}\left[\Sigma_{mpq}E^{\infty}_{pq}(0) + R_{mq}\epsilon_{qrs}(\Omega^{\infty}_r(0) - \Omega_r)x_s\right]\,\mathrm{d}S \\ &\quad - a\int_{S_p}\varepsilon f(\boldsymbol{x})\epsilon_{kln}x_l\,R^{\parallel}_{mn}(-p^{\infty}(0)n_m + \Delta^{\infty}_{ml}\big|_0\,n_l)\,\mathrm{d}S \\ &\quad - \mu\int_{S_p}\epsilon_{kln}\epsilon_{qrs}x_lx_sR_{qn}\Omega_r\,\mathrm{d}S. \end{aligned} \tag{2.21b}$$

Because $\hat{E}^B_{ij}$ and $(\hat{\Omega}^B_k - \hat{\Omega}_k)$ are independent of each other and also because (2.20) holds for arbitrary choices of $\hat{E}^B_{ij}$ and $(\hat{\Omega}^B_k - \hat{\Omega}_k)$, we can eliminate $[\hat{E}^B_{ij}, (\hat{\Omega}^B_k - \hat{\Omega}_k)]$ on both sides of (2.20), giving

$$\begin{bmatrix}\mathcal{S}_{ij}\\ \mathcal{L}_k\end{bmatrix} = \begin{bmatrix}R^E_{ij}\\ R^{\Omega}_k\end{bmatrix}. \tag{2.22}$$

As indicated by (2.21), since R^E_{ij} and R^{Ω}_k involve both $E^{\infty}_{pq}(0)$ and $(\Omega^{\infty}_r(0) - \Omega_r)$, $\mathcal{S}_{ij}$ has to further couple the rate of rotation $(\Omega^{\infty}_r(0) - \Omega_r)$, joining together with $\mathcal{L}_k$ that couples the strain rate $E^{\infty}_{pq}(0)$. This can be seen by rewriting (2.22) in a linear form of $E^{\infty}_{pq}(0)$ and $(\Omega^{\infty}_r(0) - \Omega_r)$ as follows:

$$\begin{bmatrix}\mathcal{S}_{ij}\\ \mathcal{L}_k\end{bmatrix} = \begin{bmatrix}R^{SE}_{ijpq} & R^{S\Omega}_{ijr}\\ R^{LE}_{kpq} & R^{L\Omega}_{kr}\end{bmatrix}\begin{bmatrix}E^{\infty}_{pq}(0)\\ \Omega^{\infty}_r(0) - \Omega_r\end{bmatrix} + \begin{bmatrix}\mathbb{S}^{\infty}_{ij}\\ \mathbb{L}^{\infty}_k\end{bmatrix}, \tag{2.23}$$

in which the elements on the right-hand side are

$$R^{SE}_{ijpq} = -a\mu\int_{S_p}\varepsilon f(\boldsymbol{x})\,\Sigma^{\parallel}_{mij}\Sigma_{mpq}\,\mathrm{d}S, \tag{2.24a}$$

$$R^{S\Omega}_{ijr} = -a\mu\int_{S_p}\varepsilon f(\boldsymbol{x})\,\Sigma^{\parallel}_{mij}R_{mn}\epsilon_{rsn}x_s\,\mathrm{d}S - \mu\int_{S_p}\Sigma_{nij}\epsilon_{rsn}x_s\,\mathrm{d}S, \tag{2.24b}$$

$$R^{LE}_{kpq} = -a\mu \int_{S_p} \varepsilon f(\boldsymbol{x}) \epsilon_{kln} x_l R^{\parallel}_{mn} \Sigma_{mpq} \, \mathrm{d}S, \tag{2.24c}$$

$$R^{L\Omega}_{kr} = -\mu \int_{S_p} \epsilon_{kln}\epsilon_{rsq} x_l x_s \big(a\varepsilon f(\boldsymbol{x}) R^{\parallel}_{mn} R_{mq} + R_{qn}\big) \, \mathrm{d}S, \tag{2.24d}$$

$$\begin{aligned} \mathbb{S}^{\infty}_{ij} = {} & \mu \int_{S_p} \Sigma_{mij} u^{\infty}_m \, \mathrm{d}S - a\hat{\lambda} \int_{S_p} \Sigma^{\parallel}_{mij} \sigma^{\infty}_{ml} n_l \, \mathrm{d}S \\ & - a \int_{S_p} \varepsilon f(\boldsymbol{x}) \Sigma^{\parallel}_{mij} (-p^{\infty}(0) n_m + \Delta^{\infty}_{ml}|_0 \, n_l) \, \mathrm{d}S, \end{aligned} \tag{2.24e}$$

$$\begin{aligned} \mathbb{L}^{\infty}_{k} = {} & \mu \int_{S_p} \epsilon_{kln} x_l [R_{mn} u^{\infty}_m - \epsilon_{qrs} x_s R_{qn} \Omega_r] \, \mathrm{d}S - a\hat{\lambda} \int_{S_p} \epsilon_{kln} x_l R^{\parallel}_{mn} \sigma^{\infty}_{mj} n_j \, \mathrm{d}S \\ & - a \int_{S_p} \varepsilon f(\boldsymbol{x}) \epsilon_{kln} x_l R^{\parallel}_{mn} (-p^{\infty}(0) n_m + \Delta^{\infty}_{ml}|_0 \, n_l) \, \mathrm{d}S. \end{aligned} \tag{2.24f}$$

In (2.24*b*), the second integral is identically zero. Note that the stresslet-strain tensor satisfies the symmetry $R^{SE}_{ijpq} = R^{SE}_{pqij}$. The off-diagonal coupling tensors $R^{S\Omega}_{ijk}$ and R^{LE}_{ijk} also obey the symmetry property $R^{S\Omega}_{ijk} = R^{LE}_{kji}$. Such symmetry properties between these resistance tensors are consequences of the reciprocal theorem (Hinch 1972; Masoud & Stone 2019).

To better see various contributions in (2.23), we split $(\mathcal{S}_{ij}, \mathcal{L}_k)$ into the uniform-slip part $(\mathcal{S}^{(0)}_{ij}, \mathcal{L}^{(0)}_k)$ plus the corrections $(\mathcal{S}^{(1)}_{ij}, \mathcal{L}^{(1)}_k)$ due to slip anisotropy:

$$\mathcal{S}^{(0)}_{ij} = \mu \int_{S_p} \Sigma_{mij} u^{\infty}_m \, \mathrm{d}S - a\hat{\lambda} \int_{S_p} \Sigma^{\parallel}_{mij} \sigma^{\infty}_{ml} n_l \, \mathrm{d}S, \tag{2.25a}$$

$$\begin{aligned} \mathcal{S}^{(1)}_{ij} = {} & -\varepsilon a \bigg[\int_{S_p} f(\boldsymbol{x}) \Sigma^{\parallel}_{mij} (-p^{\infty}(0) \, n_m + \Delta^{\infty}_{ml}|_0 \, n_l) \, \mathrm{d}S \\ & + \mu \int_{S_p} f(\boldsymbol{x}) \, \Sigma^{\parallel}_{mij} \Sigma_{mpq} E^{\infty}_{pq}(0) \, \mathrm{d}S \\ & + \mu \int_{S_p} f(\boldsymbol{x}) \, \Sigma^{\parallel}_{mij} R_{mn} \, \epsilon_{rsn} x_s (\Omega^{\infty}_r(0) - \Omega_r) \, \mathrm{d}S \bigg], \end{aligned} \tag{2.25b}$$

$$\mathcal{L}^{(0)}_k = \mu \int_{S_p} \epsilon_{kln} x_l \big[R_{mn} u^{\infty}_m - R_{qn} \epsilon_{qrs} \Omega_r x_s - a\hat{\lambda} R^{\parallel}_{mn} \sigma^{\infty}_{mj} n_j \big] \, \mathrm{d}S, \tag{2.25c}$$

$$\begin{aligned} \mathcal{L}^{(1)}_k = {} & -\varepsilon a \bigg[\int_{S_p} f(\boldsymbol{x}) \epsilon_{kln} x_l R^{\parallel}_{mn} (-p^{\infty}(0) \, n_m + \Delta^{\infty}_{mq}|_0 n_q) \, \mathrm{d}S \\ & + \mu \int_{S_p} f(\boldsymbol{x}) \epsilon_{kln} x_l \, R^{\parallel}_{mn} \Sigma_{mpq} E^{\infty}_{pq}(0) \, \mathrm{d}S \\ & + \mu \int_{S_p} f(\boldsymbol{x}) \epsilon_{kln} \epsilon_{rsq} x_l x_s R^{\parallel}_{mn} R_{mq} (\Omega^{\infty}_r(0) - \Omega_r) \, \mathrm{d}S \bigg]. \end{aligned} \tag{2.25d}$$

As will be shown in § 4, we will use the above formulae by expanding the slip length distribution $f(\boldsymbol{x})$ in terms of surface moments (see § 3.2) to derive the Faxén stresslet and torque relations for a non-uniform slip sphere in an arbitrary background flow.

We reiterate that the present theory is based on small slip anisotropy with $\varepsilon \ll 1$. At the opposite extreme $\varepsilon \gg 1$, this is the scenario where there is a large slip contrast on the surface of a Janus sphere partitioned by, for instance, no-slip and perfect-slip, bubble-like surfaces. In this case, since the average slip length $\hat{\lambda}$ is large, the appropriate perturbation scheme should use the amplitude of $|\lambda(\boldsymbol{x})^{-1} - \hat{\lambda}^{-1}|$ as a small parameter with respect to the large uniform slip problem that should be taken as the auxiliary problem in the reciprocal theorem formulation. Nonetheless, despite the fact that technically these two limiting scenarios are formulated differently, we expect that physically the results for $\varepsilon \gg 1$ should not differ qualitatively than those for $\varepsilon \ll 1$ in the present work.

3. Re-expressing slip anisotropy in terms of surface moments

3.1. *General considerations for constructing the stresslet of a stick–slip sphere*

To use (2.25) for computing the stresslet of a stick–slip sphere, it is more convenient to expand the spatially varying part $f(\boldsymbol{x})$ of the slip length in terms of surface harmonics (Premlata & Wei 2021). As to concerning how many terms are required to faithfully describe impacts of slip anisotropy on the stresslet, we need an additional rule, which is guided by general considerations, for constructing an anisotropic stresslet.

According to Batchelor (1970), the stresslet $\mathcal{S}_{ij}$ of a force-free particle can have two contributions. One is the common contribution from the particle exerted by the straining motion of the ambient fluid under strain rate E^{∞}_{kl}. The other is an additional contribution, which can emerge when the particle is subject to rotation at rate of $(\Omega^{\infty}_{k} - \Omega_k)$ due to an excess couple on the particle. Since $\mathcal{S}_{ij}$ has to be linear in both E^{∞}_{kl} and $(\Omega^{\infty}_{k} - \Omega_k)$, it can be constructed in the general form:

$$\mathcal{S}_{ij} = C_{ijkl}E^{\infty}_{kl} + C_{ijk}(\Omega^{\infty}_{k} - \Omega_k). \tag{3.1}$$

Here C_{ijkl} and C_{ijk} are the geometric tensors depending on the size, shape and orientation of the particle, and both are symmetrical with respect to i and j. Here C_{ijkl} is also symmetrical with respect to k and l since it can only be contracted with E^{∞}_{kl}.

Now consider a Janus sphere that possesses a stick–slip polarity in a preferential direction d_i. The geometric tensors in (3.1) can then be constructed below in terms of d_i by satisfying the above-mentioned symmetry classes,

$$C_{ijkl} = \alpha_0\delta_{ik}\delta_{jl} + \alpha_1(d_id_k\delta_{jl} + d_jd_k\delta_{il}) + \alpha_2 d_id_jd_kd_l, \tag{3.2a}$$

$$C_{ijk} = \alpha_3(\epsilon_{ikm}d_j + \epsilon_{jkm}d_i)d_m, \tag{3.2b}$$

with α_0, α_1, α_2 and α_3 being the scalar coefficients.

With (3.2), (3.1) becomes

$$\mathcal{S}_{ij} = \alpha_0E^{\infty}_{ij} + \alpha_1(d_id_kE^{\infty}_{kj} + d_jd_kE^{\infty}_{ki}) + \alpha_2 d_id_jd_kd_lE^{\infty}_{kl} + \alpha_3(\epsilon_{ikm}d_j + \epsilon_{jkm}d_i)d_m(\Omega^{\infty}_{k} - \Omega_k), \tag{3.3}$$

which furnishes the general expression for the stresslet of a stick–slip sphere. As in Nir & Acrivos (1973) and Ramachandran & Khair (2009), this general stresslet expression is made only of d_pd_q and $d_id_jd_kd_l$, although the last term in (3.3) due to rotation is not included in these previous studies. Since d_pd_q can be described by surface quadrupole corresponding to the second surface harmonics (Anderson 1985; Premlata & Wei 2021), $d_id_jd_kd_l$ can only be captured by a surface hexadecapole, two orders higher than the former.

In other words, to describe the stresslet in the form (3.3) it is necessary to keep at least the first four surface harmonics in the harmonics expansion of the slip length, which will be presented in the next subsection.

It is worth mentioning that involving only $d_p d_q$ and $d_i d_j d_k d_l$ in the construction of the stresslet (3.3) can be understood using a symmetry argument. This is because they are the only polyadic combinations using d_i that can work with E_{ij}^{∞} and $(\Omega_k^{\infty} - \Omega_k)$ to form a stresslet that is a symmetric second-order tensor. It is thus impossible to use d_i alone to make such a construction. It follows that surface dipole will make no contribution to the stresslet in a linear flow field. That is, if the sphere is half-faced with a dipole only, its stresslet will show no difference than the uniform-slip one.

3.2. *Surface spherical harmonics expansion*

Following Premlata & Wei (2021), we expand the spatially varying slip length $\lambda(\boldsymbol{x})$ as a series of surface spherical harmonics,

$$\lambda(\boldsymbol{x}) = \sum_m (a/r)^{m+1} G_m[\cdot] \boldsymbol{S}_m, \tag{3.4}$$

where the mth-order polyadic $\boldsymbol{S}_m$ denotes surface spherical harmonics,

$$\boldsymbol{S}_m \equiv r^{m+1} (\boldsymbol{\nabla} \cdots \boldsymbol{\nabla})^m \left(r^{-1} \right), \tag{3.5}$$

with G_m being the coefficients to form a scalar product with $\boldsymbol{S}_m$ through operator $[\cdot]$. As mentioned in § 3.1, it is necessary to keep the terms at least to $m = 4$, requiring the following harmonics for determining the stresslet of a stick–slip sphere:

$$\left.\begin{aligned} S_0 &= 1, \\ S_{1i} &= -n_i, \\ S_{2ij} &= 3n_i n_j - \delta_{ij}, \\ S_{3ijk} &= -15 n_i n_j n_k + 3(n_i \delta_{jk} + n_j \delta_{ik} + n_k \delta_{ij}), \\ S_{4ijkl} &= 105 n_i n_j n_k n_l + 3(\delta_{ij}\delta_{kl} + \delta_{ik}\delta_{jl} + \delta_{il}\delta_{jk}) \\ &\quad - 15(n_i n_j \delta_{kl} + n_i n_k \delta_{jl} + n_i n_l \delta_{jk} + n_j n_k \delta_{il} + n_j n_l \delta_{ik} + n_k n_l \delta_{ij}). \end{aligned}\right\} \tag{3.6}$$

To determine the coefficients G_m in (3.4), the orthogonal relationships between distinct surface harmonics are needed,

$$\langle \boldsymbol{S}_m \boldsymbol{S}_k \rangle = 1/\left(4\pi a^2\right) \int_{Sp} \boldsymbol{S}_m \boldsymbol{S}_k \, \mathrm{d}S, \tag{3.7}$$

with $\langle\cdots\rangle = 1/(4\pi a^2)\int_{S_p}(\cdots)\,\mathrm{d}S$ denoting the average over the sphere's surface. The orthogonal relationships for the required surface harmonics (3.6) are given by

$$\left.\begin{aligned}
\langle S_0 S_0\rangle &= 1,\\
\langle \boldsymbol{S}_1\boldsymbol{S}_1\rangle_{ij} &= \frac{1}{3}\delta_{ij},\\
\langle \boldsymbol{S}_2\boldsymbol{S}_2\rangle_{ijkl} &= \frac{1}{5}\left(-2\delta_{ij}\delta_{kl}+3\delta_{ik}\delta_{jl}+3\delta_{il}\delta_{jk}\right),\\
\langle \boldsymbol{S}_3\boldsymbol{S}_3\rangle_{ijkpql} &= \frac{15}{7}\left(\delta_{ij}A_{pqkl}+\delta_{ik}A_{pqjl}+\delta_{ip}A_{jklq}+\delta_{iq}A_{jklp}+\delta_{il}A_{jkpq}\right)\\
&\quad -3\left(\delta_{pq}A_{ijkl}+\delta_{pl}A_{ijkq}+\delta_{ql}A_{ijkp}\right),\\
\langle \boldsymbol{S}_4\boldsymbol{S}_4\rangle_{ijklpqrs} &= \frac{35}{3}\left[C_{ijklpqrs}+\frac{9}{5}A_{ijkl}A_{pqrs}+\frac{9}{7}(\delta_{rs}B_{ijklpq}+\delta_{qs}B_{ijklpr}\right.\\
&\quad \left.+\delta_{qr}B_{ijklps}+\delta_{ps}B_{ijklqr}+\delta_{pr}B_{ijklqs}+\delta_{pq}B_{ijklrs})\right].
\end{aligned}\right\} \tag{3.8}$$

In the above, $A_{ijkm}=\delta_{ij}\delta_{km}+\delta_{ik}\delta_{jm}+\delta_{im}\delta_{jk}$, $B_{pqijkm}=\delta_{pq}A_{ijkm}+\delta_{pi}A_{qjkm}+\delta_{pj}A_{iqkm}+\delta_{pk}A_{ijqm}+\delta_{pm}A_{ijkq}$ and $C_{pqijkmnl}=\delta_{km}B_{pqijnl}+\delta_{kn}B_{pqijml}+\delta_{kl}B_{pqijnm}+\delta_{kp}B_{mqijnl}+\delta_{kq}B_{pmijnl}+\delta_{ki}B_{pqmjnl}+\delta_{kj}B_{pqimnl}$.

Applying (3.8) to (3.4) and knowing that monopole $\langle\lambda S_0\rangle=\langle\lambda\rangle(=\hat{\lambda})$ is simply the average slip length, we can decompose the slip variation part into a superposition of surface moments by retaining at least the first four ones: dipole $\boldsymbol{P}_1\equiv-\langle\lambda\boldsymbol{S}_1\rangle$; quadrupole $\boldsymbol{P}_2\equiv\langle\lambda\boldsymbol{S}_2\rangle$; octupole $\boldsymbol{P}_3\equiv-\langle\lambda\boldsymbol{S}_3\rangle$; hexadecapole $\boldsymbol{P}_4\equiv\langle\lambda\boldsymbol{S}_4\rangle$ etc.: $\lambda'(\boldsymbol{y})=\langle\lambda\rangle-3\boldsymbol{P}_1\cdot\boldsymbol{S}_1+(5/6)\boldsymbol{P}_2:\boldsymbol{S}_2+\cdots$, etc., giving

$$\varepsilon f(\boldsymbol{x}) = -3P_{1i}S_{1i}+(5/6)P_{2ij}S_{2ij}-(7/90)P_{3ijk}S_{3ijk}+(1/280)P_{4ijkl}S_{4ijkl}+\cdots. \tag{3.9}$$

The surface moments $\boldsymbol{P}_1$, $\boldsymbol{P}_2$, $\boldsymbol{P}_3$ and $\boldsymbol{P}_4$ in (3.9) can be written in terms the stick–slip director $\boldsymbol{d}$ with the corresponding strengths $\mathcal{D}$, $\mathcal{Q}$, $\mathcal{O}$ and $\mathcal{H}$:

$$P_{1i} = \mathcal{D}d_i, \tag{3.10a}$$

$$P_{2ij} = \mathcal{Q}(3d_id_j-\delta_{ij}), \tag{3.10b}$$

$$P_{3ijk} = 3\mathcal{O}(5d_id_jd_k-d_i\delta_{jk}-d_j\delta_{ik}-d_k\delta_{ij}), \tag{3.10c}$$

$$\begin{aligned}P_{4ijkl} = 3\mathcal{H}\big[&35d_id_jd_kd_l+\delta_{ij}\delta_{lk}+\delta_{ik}\delta_{jl}+\delta_{il}\delta_{jk}\\ &-5(d_id_j\delta_{kl}+d_id_k\delta_{jl}+d_id_l\delta_{jk}+d_jd_k\delta_{il}+d_jd_l\delta_{ik}+d_kd_l\delta_{ij})\big].\end{aligned} \tag{3.10d}$$

As illustrated in figure 2, the above surface moments represent distinct symmetries of stick–slip patterns. Dipole $\boldsymbol{P}_1$ is the first odd mode. It can be pictured as a half-faced stick–slip pattern characterized by the director $\boldsymbol{d}$ pointing from the stick face to the slip face (with $\mathcal{D}>0$). Quadrupole $\boldsymbol{P}_2$ is the first even mode, representing a symmetric slip–stick–slip (with $\mathcal{Q}>0$) (or stick–slip–stick with $\mathcal{Q}<0$) pattern of striped type. Octupole $\boldsymbol{P}_3$ is the second odd mode, made of two antisymmetric hemispheres with stripes. Hexadecapole $\boldsymbol{P}_4$ is the second even mode, represented by symmetric caps with an alike stripe in the middle.

Substitution of (3.9) into (2.25) will allow us to systematically quantify impacts of slip anisotropy on $\mathcal{S}_{ij}$ and $\mathcal{L}_k$ in terms of the surface moments above.

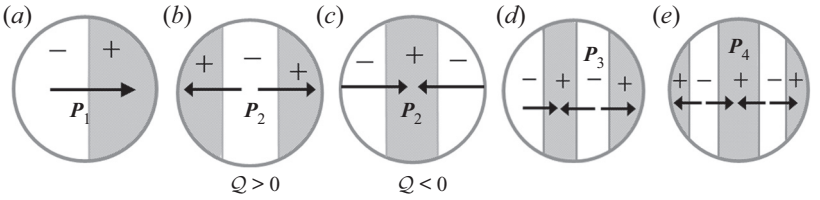

Figure 2. Schematic illustrations of the first four surface moments. Dipole $\boldsymbol{P}_1$ can be pictured as a half-faced stick–slip pattern. Quadrupole $\boldsymbol{P}_2$ can be thought of as a symmetric slip–stick–slip ($\mathcal{Q} > 0$) or stick–slip–stick ($\mathcal{Q} < 0$) pattern of striped type. Octupole $\boldsymbol{P}_3$ can be represented by two antisymmetric hemispheres with stripes. Hexadecapole $\boldsymbol{P}_4$ can be deemed as a pattern possessing symmetric caps with an alike stripe in the middle.

To see how the strengths of surface moments are determined for a given axisymmetric slip length distribution, we rewrite (3.9) in terms of the stick–slip director $\boldsymbol{d}$:

$$\varepsilon f(\boldsymbol{x}) = -3\mathcal{D}d_iS_{1i} + (5/2)\mathcal{Q}d_id_jS_{2ij} - (7/6)Od_id_jd_kS_{3ijk} + (3/8)\mathcal{H}d_id_jd_kd_lS_{4ijkl} + \cdots. \tag{3.11}$$

In deriving (3.11) we have used the fact that these surface moments are zero when any two indices are identical, namely, $S_{2ij}\delta_{ij}$, $S_{3ijk}\delta_{ij}$ and $S_{4ijkl}\delta_{ij}$ are zero. Also note that $\mathcal{D}$, $\mathcal{Q}$, $\mathcal{O}$ and $\mathcal{H}$ are $O(\varepsilon)$ because of $\varepsilon f(\boldsymbol{x})$ in (3.11).

Equation (3.11) plus $\langle\lambda\rangle$ should be equal to the form by expanding the slip length to a Legendre series:

$$\lambda(\eta) = a_0\mathcal{P}_0(\eta) + a_1\mathcal{P}_1(\eta) + a_2\mathcal{P}_2(\eta) + a_3\mathcal{P}_3(\eta) + a_4\mathcal{P}_4(\eta) + \cdots. \tag{3.12}$$

Here $\mathcal{P}_0(\eta) = 1, \mathcal{P}_1(\eta) = \eta, \mathcal{P}_2(\eta) = (3\eta^2 - 1)/2, \mathcal{P}_3(\eta) = (5\eta^3 - 3\eta)/2, \mathcal{P}_4(\eta) = (35\eta^4 - 30\eta^2 + 3)/8$, etc. are the Legendre polynomials with $\eta = \cos\theta$ in terms of the polar angle θ with respect to the symmetry axis and the coefficients a_n are given by $a_n = (n + 1/2)\int_{-1}^{1}\lambda\mathcal{P}_n(\eta)\,\mathrm{d}\eta$. Comparing (3.12) with (3.11), we can determine the strengths of surface moments in terms of a_n (see Appendix A):

$$\langle\lambda\rangle = a_0, \mathcal{D} = a_1/3, \mathcal{Q} = a_2/5, O = a_3/7 \text{ and } \mathcal{H} = a_4/9. \tag{3.13}$$

Take a commonly prepared two-faced Janus sphere having slip lengths λ^+ and λ^- as an example (see figure 3). With the aid of (3.13), the strengths of surface moments can be readily found:

$$\langle\lambda\rangle = (1/2)(\lambda^+ + \lambda^- - (\lambda^+ - \lambda^-)\cos\alpha), \tag{3.14a}$$

$$\mathcal{D} = (1/4)(\lambda^+ - \lambda^-)\sin^2\alpha, \tag{3.14b}$$

$$\mathcal{Q} = (1/4)(\lambda^+ - \lambda^-)\sin^2\alpha\cos\alpha, \tag{3.14c}$$

$$O = (1/16)(\lambda^+ - \lambda^-)\sin^2\alpha(5\cos^2\alpha - 1), \tag{3.14d}$$

$$\mathcal{H} = (1/16)(\lambda^+ - \lambda^-)\sin^2\alpha\cos\alpha(7\cos^2\alpha - 3), \tag{3.14e}$$

where α is the stick–slip division angle for the more slippery λ^+ part. As indicated by (3.14), the strengths of these surface moments are proportional to the stick–slip contrast $(\lambda^+ - \lambda^-)$ modulated by the stick–slip division angle α.

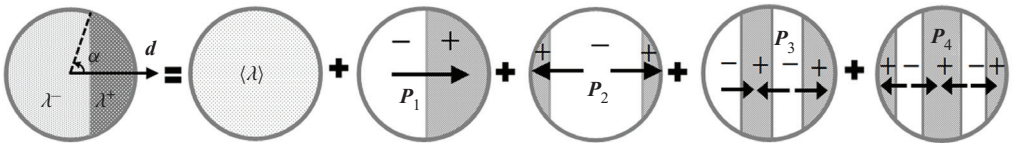

Figure 3. The slip length distribution of a stick–slip Janus sphere can be represented by its average slip length plus a linear combination of various surface moments listed in figure 2.

4. Extended Faxén relations for anisotropic stresslet and torque on a stick–slip sphere

To evaluate $\mathcal{S}_{ij}$ and $\mathcal{L}_k$ from (2.25), first of all we need the strain resistance tensor Σ_{mij} and the rotation resistance tensor R_{ij} for the uniform-slip problem:

$$\Sigma_{mij} = \frac{5}{1+5\hat{\lambda}}\delta_{im}n_j + \frac{40\hat{\lambda}}{1+5\hat{\lambda}}n_m n_i n_j, \tag{4.1a}$$

$$R_{ij} = \frac{3/a}{(1+3\hat{\lambda})}\delta_{ij}. \tag{4.1b}$$

Next, we expand $\boldsymbol{u}^\infty$ and $\boldsymbol{\sigma}^\infty$ with respect to the sphere's centre located at $\boldsymbol{x}=0$ as

$$u_i^\infty = u_i^\infty(0) + x_j\nabla_j u_i^\infty\big|_0 + \frac{x_j x_k}{2!}\nabla_j\nabla_k u_i^\infty\big|_0 + \cdots, \tag{4.2a}$$

$$\sigma_{im}^\infty = \sigma_{im}^\infty(0) + x_j\nabla_j \sigma_{im}^\infty\big|_0 + \frac{x_j x_k}{2!}\nabla_j\nabla_k \sigma_{im}^\infty\big|_0 + \cdots. \tag{4.2b}$$

Substituting (3.9), (4.1) and (4.2) into (2.25), we are able to compute $\mathcal{S}_{ij}$ and $\mathcal{L}_k$ on a stick–slip sphere. Their evaluations, which are given in Appendices B and C, can be implemented with the aid of the following surface integrals involving even numbers of surface normal vector $\boldsymbol{n}$:

$$\int_{S_p} n_i n_j \,\mathrm{d}S = (4/3)\pi a^2\delta_{ij}, \tag{4.3a}$$

$$\int_{S_p} n_i n_j n_k n_m \,\mathrm{d}S = (4/15)\pi a^2 A_{ijkm}, \tag{4.3b}$$

$$\int_{S_p} n_p n_q n_i n_j n_k n_m \,\mathrm{d}S = (4/105)\pi a^2 B_{pqijkm}, \tag{4.3c}$$

$$\int_{S_p} n_p n_q n_i n_j n_k n_m n_n n_l \,\mathrm{d}S = (4/945)\pi a^2 C_{pqijkmnl}, \tag{4.3d}$$

where A_{ijkm}, B_{pqijkm} and $C_{pqijkml}$ are defined in (3.8).

4.1. *Stresslet*

Here we merely present the end results after evaluating the stresslet using (2.25*a*,*b*). The detailed evaluations of relevant contributions to the stresslet can be found in Appendix B. The surface monopole measures the average slip length. The associated stresslet is

represented by the uniform-slip part (2.25*a*), which gives

$$\mathcal{S}_{ij}^{(0)} = \frac{20}{3}\left(\frac{1+2\hat{\lambda}}{1+5\hat{\lambda}}\right)\pi\mu a^3 E_{ij}^{\infty}\big|_0 + \frac{2}{3}\left(\frac{1}{1+5\hat{\lambda}}\right)\pi\mu a^5 \nabla^2 E_{ij}^{\infty}\big|_0, \tag{4.4}$$

which recovers the result obtained by Keh & Chen (1996) for a uniform-slip sphere.

The $O(\varepsilon)$ slip anisotropy correction (2.25*b*) comprises surface dipole, quadrupole, octupole and hexadecapole contributions, $\mathcal{S}_{ij}^{(1)} = \mathcal{S}_{ij}^{D} + \mathcal{S}_{ij}^{Q} + \mathcal{S}_{ij}^{O} + \mathcal{S}_{ij}^{H}$, modifying the stresslet according to

$$\begin{aligned}
\mathcal{S}_{ij}^{D} &= -3a\langle\lambda S_{1k}\rangle \int_{S_p} S_{1k}\Sigma_{mij}^{\parallel}(-p^{\infty}(0)n_m + x_p\nabla_p\sigma_{ml}^{\infty}\big|_0 n_l + \cdots)\,\mathrm{d}S \\
&= -\frac{40/7}{1+5\hat{\lambda}}\pi\mu a^4\left(1+\frac{7a^2}{90}\nabla^2\right)\nabla_k E_{ij}^{\infty}\big|_0 P_{1k} \\
&\quad - \frac{12/7}{1+5\hat{\lambda}}\pi\mu a^4 P_{1k}\Big[\nabla_i E_{jk}^{\infty}\big|_0 + \nabla_j E_{ik}^{\infty}\big|_0 + \nabla_m E_{jm}^{\infty}\big|_0\delta_{ik} + \nabla_m E_{im}^{\infty}\big|_0\delta_{jk} \\
&\quad - \frac{4}{3}\delta_{ij}\nabla_l E_{lk}^{\infty}\big|_0\Big],
\end{aligned} \tag{4.5a}$$

$$\begin{aligned}
\mathcal{S}_{ij}^{Q} &= -a(5/6)\langle\lambda S_{2pq}\rangle\Big[\mu\int_{S_p} S_{2pq}\Sigma_{mij}^{\parallel}\Sigma_{mlk}\,E_{lk}^{\infty}(0)\,\mathrm{d}S \\
&\quad + \mu\int_{S_p} S_{2pq}\,\Sigma_{mij}^{\parallel}R_{mn}\epsilon_{rsn}x_s(\Omega_r^{\infty}(0)-\Omega_r)\,\mathrm{d}S \\
&\quad + \int_{S_p} S_{2pq}\,\Sigma_{mij}^{\parallel}(-p^{\infty}(0)n_m + \frac{x_n x_k}{2!}\nabla_n\nabla_k\sigma_{ml}^{\infty}\big|_0 n_l)\,\mathrm{d}S\Big] \\
&= -\frac{50/7}{(1+5\hat{\lambda})^2}\pi\mu a^3\Big[E_{jp}^{\infty}\big|_0 P_{2ip} + E_{ip}^{\infty}\big|_0 P_{2jp} - \frac{2}{3}\delta_{ij}E_{pq}^{\infty}\big|_0 P_{2pq}\Big] \\
&\quad - \frac{10}{(1+3\hat{\lambda})(1+5\hat{\lambda})}\,\pi\mu a^3\left[\epsilon_{irp}P_{2jp} + \epsilon_{jrp}P_{2ip}\right](\Omega_r^{\infty}(0)-\Omega_r) \\
&\quad - \frac{20/189}{1+5\hat{\lambda}}\pi\mu a^5 P_{2pq}\Big[5\nabla_p\nabla_k(E_{jq}^{\infty}\big|_0\delta_{ik} + E_{iq}^{\infty}\big|_0\delta_{jk}) + 3\nabla^2\left(E_{jq}^{\infty}\big|_0\delta_{ip} + E_{iq}^{\infty}\big|_0\delta_{jp}\right) \\
&\quad - 3\nabla^2 E_{pq}^{\infty}\big|_0\delta_{ij} - 2\nabla_i\nabla_j E_{pq}^{\infty}\big|_0 + 7\nabla_p\nabla_q E_{ij}^{\infty}\big|_0\Big],
\end{aligned} \tag{4.5b}$$

$$\begin{aligned}
\mathcal{S}_{ij}^{O} &= -a(7/90)\langle\lambda S_{3kpq}\rangle\int_{S_p} S_{3kpq}\Sigma_{mij}^{\parallel}(-p^{\infty}(0)\,n_m + x_n\nabla_n\sigma_{ml}^{\infty}\big|_0\,n_l + \cdots)\,\mathrm{d}S \\
&= -\frac{8/27}{1+5\hat{\lambda}}\mu\pi a^4\Big[2\nabla_k E_{nk}^{\infty}\big|_0 P_{3ijn} + \delta_{ij}\nabla_l E_{mn}^{\infty}\big|_0 P_{3mnl} + \nabla_j E_{mn}^{\infty}\big|_0 P_{3imn} + \nabla_i E_{mn}^{\infty}\big|_0 P_{3jmn} \\
&\quad - \frac{5}{2}(\nabla_n E_{jm}^{\infty}\big|_0 P_{3imn} + \nabla_n E_{im}^{\infty}\big|_0 P_{3jmn})\Big],
\end{aligned} \tag{4.5c}$$

$$\mathcal{S}_{ij}^{H} = -a\mu(1/280)\left\langle \lambda S_{4pqrs}\right\rangle \int_{S_p} S_{4pqrs}\ \Sigma_{mij}^{\parallel}\Sigma_{mlk}\ E_{lk}^{\infty}(0)\,\mathrm{d}S$$
$$= \frac{20/21}{(1+5\hat{\lambda})^2}\pi\mu a^3 P_{4ijlk}E_{lk}^{\infty}(0). \tag{4.5d}$$

Note that the stresslet–rotation coupling $(\Omega_r^{\infty}(0)-\Omega_r)$ term comes from $\mathcal{S}_{ij}^{Q}$ in (4.5*b*). Combining (4.4)–(4.5) gives the extended Faxén stresslet relation,

$$\mathcal{S}_{ij} = \frac{20}{3}\pi\mu a^3\left(\frac{1+2\hat{\lambda}}{1+5\hat{\lambda}}\right)\left[1+\frac{a^2}{10(1+2\hat{\lambda})}\nabla^2\right]E_{ij}^{\infty}\big|_0 + \pi\mu a^3 J_{3ij} + \pi\mu a^4 J_{4ij} + \pi\mu a^5 J_{5ij}, \tag{4.6a}$$

where various finite-size anisotropic contributions from surface moments can be summed up below according to their associations with different powers of a:

$$J_{3ij} = \frac{20/21}{(1+5\hat{\lambda})^2}P_{4ijkl}E_{kl}^{\infty}\big|_0$$
$$-\frac{10}{(1+3\hat{\lambda})(1+5\hat{\lambda})}P_{2pq}\left[\delta_{jq}\epsilon_{irp}+\delta_{iq}\epsilon_{jrp}\right](\Omega_r^{\infty}(0)-\Omega_r)$$
$$-\frac{50/7}{(1+5\hat{\lambda})^2}P_{2pq}\left[\delta_{iq}E_{jp}^{\infty}\big|_0+\delta_{jq}E_{ip}^{\infty}\big|_0-\frac{2}{3}E_{pq}^{\infty}\big|_0\delta_{ij}\right], \tag{4.6b}$$

$$J_{4ij} = -\frac{40/7}{1+5\hat{\lambda}}P_{1k}\nabla_k E_{ij}^{\infty}$$
$$-\frac{12/7}{1+5\hat{\lambda}}P_{1k}\left[\nabla_i E_{jk}^{\infty}\big|_0+\nabla_j E_{ik}^{\infty}\big|_0+\delta_{ik}\nabla_m E_{jm}^{\infty}\big|_0+\delta_{jk}\nabla_m E_{im}^{\infty}\big|_0-\frac{4}{3}\delta_{ij}\nabla_m E_{mk}^{\infty}\big|_0\right]$$
$$-\frac{8/27}{1+5\hat{\lambda}}P_{3mnl}\left[\frac{5}{2}\nabla_l(E_{jm}^{\infty}\big|_0\delta_{in}+E_{im}^{\infty}\big|_0\delta_{jn}-\frac{2}{5}E_{mn}^{\infty}\big|_0\delta_{ij})-(\nabla_j E_{mn}^{\infty}\big|_0\delta_{il}\right.$$
$$\left.+\nabla_i E_{mn}^{\infty}\big|_0\delta_{jl})-2\nabla_k E_{lk}^{\infty}\big|_0\delta_{in}\delta_{jm}\right], \tag{4.6c}$$

$$J_{5ij} = -\frac{20/189}{1+5\hat{\lambda}}P_{2pq}\left[5\nabla_p(\nabla_i E_{jq}^{\infty}\big|_0+\nabla_j E_{iq}^{\infty}\big|_0)+3\nabla^2\left(E_{jq}^{\infty}\big|_0\delta_{ip}+E_{iq}^{\infty}\big|_0\delta_{jp}\right)\right.$$
$$\left.-3\nabla^2 E_{pq}^{\infty}\big|_0\delta_{ij}-2\nabla_i\nabla_j E_{pq}^{\infty}\big|_0+7\nabla_p\nabla_q E_{ij}^{\infty}\big|_0\right]. \tag{4.6d}$$

Here a variety of anisotropic stresslet contributions ((4.6*b*)–(4.6*d*)) are written in the traceless form to ensure the total stresslet (4.6*a*) is trace-free. As indicated by (4.6*a*), in a linear flow field the impacts of slip anisotropy on the stresslet are reflected purely by symmetric quadrupole $\boldsymbol{P}_2$ and hexadecapole $\boldsymbol{P}_4$. The Faxén corrections with the a^5 terms also come from these symmetric surface moments when the imposed flow is of a cubic type or of a higher degree. Antisymmetric dipole $\boldsymbol{P}_1$ and octupole $\boldsymbol{P}_3$ affect the stresslet through the finite-size a^4 terms if the imposed strain rate is non-uniform.

While the variety of terms associated with distinct surface moments in (4.6*b*)–(4.6*d*) may look complicated, each in fact takes a unique and specific form as computed. They can be obtained below using simple tensor constructions guided by the linearity of Stokes flow. For simplicity, we only present canonical forms in the constructions by

omitting the associated symmetric parts which can be easy to obtain by interchanging the indices.

First consider the contributions from even surface moments. For quadrupole P_{2ik}, constructing a stresslet $\mathcal{S}_{ij}$ with P_{2ik} in a purely straining field E^{∞}_{kj} can only be done with $\mathcal{S}_{ij} = P_{2ik}E^{\infty}_{kj}$. Similarly, that in a purely rotating field Ω^{∞}_{r} can only be constructed as $\epsilon_{jrk}P_{2ik}\Omega^{\infty}_{r}$. These contributions can be seen in (4.6*b*). As for the Faxén stresslet corrections due to P_{2ik}, the admissible forms can only be $P_{2ik}\nabla^2 E^{\infty}_{jk}$ and $P_{2lk}\nabla_l\nabla_i E^{\infty}_{jk}$, by having $P_{2ik}E^{\infty}_{kj}$ operated under differential operators, as obtained in (4.6*d*). For hexadecapole P_{4ijkl}, $\mathcal{S}_{ij}$ can only be made in the form of $P_{4ijkl}E^{\infty}_{kl}$, as shown in (4.6*b*).

For the contributions from odd surface moments, dipole P_{1k} cannot work with a strain field E^{∞}_{ij} but with a field gradient $\nabla_k E^{\infty}_{ij}$ to yield a stresslet $P_{1k}\nabla_k E^{\infty}_{ij}$ or $P_{1k}\nabla_i E^{\infty}_{jk}$, as derived in (4.6*c*). Similarly, octupole P_{3ilk} can make a contribution $P_{3ilk}\nabla_k E^{\infty}_{jl}$, $P_{3ijk}\nabla_l E^{\infty}_{lk}$ or $\nabla_j P_{3ilk}E^{\infty}_{lk}$ to $\mathcal{S}_{ij}$ when it joins a field gradient $\nabla_k E^{\infty}_{ij}$ or $\nabla_l E^{\infty}_{lk}$, as obtained in (4.6*c*).

Now return to the total stresslet (4.6*a*). Since (4.6*a*) contains both the $O(\varepsilon)$ slip anisotropy corrections and the finite-size correction terms of $O((a/L)^2)$ and smaller (with L being the macroscopic length over which flow gradients occur), the former can be more important than the latter if the imposed flow is linear or

$$\varepsilon \gg (a/L)^2. \tag{4.7}$$

Under the above condition, we can neglect the finite-size correction terms $\nabla^2\boldsymbol{E}^{\infty}|_0$, $\boldsymbol{P}_1 \cdot \nabla\boldsymbol{E}^{\infty}|_0$, $\nabla(\boldsymbol{E}^{\infty}|_0 \cdot \boldsymbol{P}_1)$, $\boldsymbol{P}_2 : \nabla\nabla\boldsymbol{E}^{\infty}|_0$, $\nabla^2\boldsymbol{E}^{\infty}|_0 \cdot \boldsymbol{P}_2$, $\nabla \cdot (\boldsymbol{P}_3 \cdot \boldsymbol{E}^{\infty}|_0)$, $\boldsymbol{P}_3 \cdot (\nabla \cdot \boldsymbol{E}^{\infty}|_0)$, $\nabla(\boldsymbol{P}_3 : \boldsymbol{E}^{\infty}|_0)$ due to the non-uniformity of the imposed strain field, simplifying (4.6*a*) to

$$\frac{\mathcal{S}_{ij}}{\pi\mu a^3} = \frac{20}{3}\left(\frac{1+2\hat{\lambda}}{1+5\hat{\lambda}}\right)E^{\infty}_{ij}\big|_0 - \frac{50/7}{(1+5\hat{\lambda})^2}\left[P_{2ip}E^{\infty}_{jp}\big|_0 + P_{2jp}E^{\infty}_{ip}\big|_0 - (2/3)P_{2pq}E^{\infty}_{pq}\big|_0\delta_{ij}\right]$$
$$+ \frac{20/21}{(1+5\hat{\lambda})^2}P_{4ijlk}E^{\infty}_{lk}\big|_0 - \frac{10}{(1+3\hat{\lambda})(1+5\hat{\lambda})}[\epsilon_{irp}P_{2jp} + \epsilon_{jrp}P_{2ip}](\Omega^{\infty}_{r}(0) - \Omega_r). \tag{4.8}$$

It is exactly the general stresslet expression (3.3) when writing quadrupole P_{2pq} and hexadecapole P_{4ijlk} back to $d_p d_q$ and $d_i d_j d_l d_k$ using (3.10*b*) and (3.10*d*), as can be seen from (5.4) later.

Equation (4.8) reveals that the anisotropic part of stresslet in a linear flow field is determined purely from symmetric P_{2pq} and P_{4ijlk}. Note that while these two surface moments contribute to the stresslet in a purely straining field, stresslet–rotation coupling arises only from P_{2pq}. In figure 4 we use a slip–stick–slip sphere whose stick–slip pattern can be represented by P_{2pq} to illustrate how stresslets are generated from asymmetric forces around the sphere in linear flow fields. Figure 4(*b*,*c*) display how these forces turn into a stresslet and a couple under the actions of a purely straining flow field and those of a purely rotating flow field, respectively. In the latter case, a stresslet can result from the vorticity of an imposed flow or from body rotation, giving rise to the stresslet–rotation coupling term in (4.8) (figure 4*c*). Likewise, a couple can be generated by applying a strain field to the sphere, resulting in torque-strain coupling (figure 4*b*). Compared with the usual no-slip case (figure 4*a*), the main difference is that asymmetric forces on the sphere lead the resulting force pair to be unaligned with respect to the sphere's centre, acting as a symmetric stresslet and an antisymmetric couple across the sphere.

For a Janus sphere whose stick–slip pattern is purely antisymmetric like an equally divided face represented by dipole P_{1k}, slip anisotropy will make no contribution to the stresslet until $O(\varepsilon^2)$. The anisotropic stresslet of such sphere can only be seen by placing

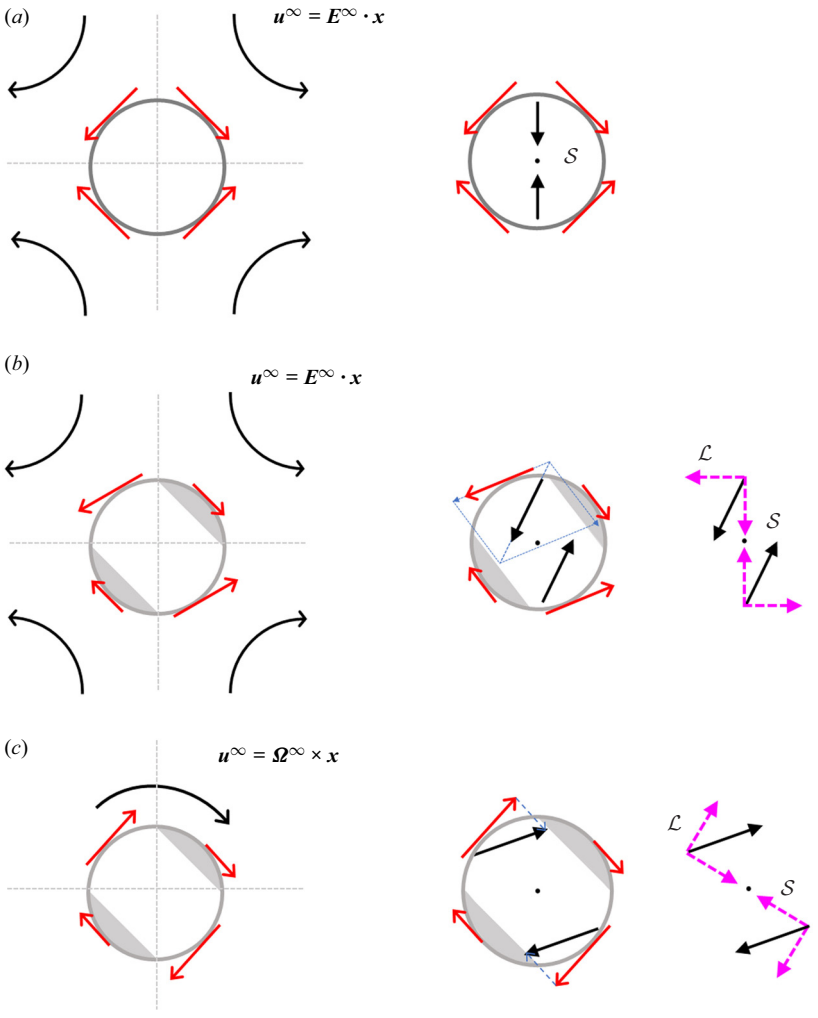

Figure 4. Schematic cartoons showing the use of a slip–stick–slip sphere for illustrating how different anisotropic stresslet contributions form due to surface quadrupole in a linear flow field in comparison with the usual no-slip case (*a*). Panel (*b*) illustrates the situation in a purely straining flow field, showing how asymmetric forces (red arrows) form around the sphere due to the slip asymmetry. These forces then produce a force pair that acts as a symmetric stresslet and an antisymmetric couple across the sphere. The couple is responsible for the torque-strain coupling term in (4.12). Panel (*c*) displays the similar situation in a purely rotating flow field, explaining how the stresslet–rotation coupling term in (4.8) arises from the vorticity of an imposed flow or from body rotation.

the sphere in a nonlinear flow field in which the a^4 terms in (4.6*a*) can emerge due to antisymmetric dipole P_{1k} or/and octupole P_{3kpq}.

4.2. *Torque*

As indicated by (4.6*a*), the stresslet of a stick–slip sphere can further couple to its rotational motion. To find the rate of rotation for the sphere, we need to determine the hydrodynamic torque on the sphere. Again, we present the end results by leaving the detailed derivations

to Appendix C. The uniform-slip part (2.25*c*) of the torque is

$$\mathcal{L}_k^{(0)} = \frac{8}{1+3\hat{\lambda}}\pi\mu a^3(\Omega_k^\infty(0) - \Omega_k), \tag{4.9}$$

which again agrees with the result obtained by Keh & Chen (1996) for a uniform-slip sphere. Similar to the stresslet (4.6*a*), the slip anisotropy correction (2.25*d*) is found to consist of surface dipole, quadrupole and octupole contributions, $\mathcal{L}_k^{(1)} = \mathcal{L}_k^D + \mathcal{L}_k^Q + \mathcal{L}_k^O$, as computed as follows:

$$\begin{aligned}
\mathcal{L}_k^D &= -3a\langle\lambda S_{1j}\rangle \int_{S_p} S_{1j}\epsilon_{kln}x_l R_{mn}^{\parallel}(-p^\infty(0)\, n_m + x_p\nabla_p\sigma_{mq}^\infty(0)\, n_q + \cdots)\mathrm{d}S \\
&= -\frac{24/5}{1+3\hat{\lambda}}\pi\mu a^4\epsilon_{kmn}(\nabla_m E_{jn}^\infty\big|_0 P_{1j} - \nabla_p E_{pm}^\infty\big|_0 P_{1n}), \qquad (4.10a) \\
\mathcal{L}_k^Q &= -a(5/6)\langle\lambda S_{2ij}\rangle\left[\int_{S_p} S_{2ij}\epsilon_{kln}x_l R_{mn}^{\parallel}\Sigma_{mpq}E_{pq}^\infty(0)\,\mathrm{d}S\right. \\
&\quad + \mu\int_{S_p} S_{2ij}\epsilon_{kln}\epsilon_{rsq}x_l x_s R_{mn}^{\parallel}R_{mq}(\Omega_r^\infty(0) - \Omega_r)\,\mathrm{d}S \\
&\quad \left. + \int_{S_p} S_{2ij}\epsilon_{kln}x_l\, R_{mn}^{\parallel}(-p^\infty(0)n_m + \frac{x_p x_q}{2!}\nabla_p\nabla_q\sigma_{mr}^\infty\big|_0 n_r + \cdots)\,\mathrm{d}S\right] \\
&= -\frac{20}{(1+3\hat{\lambda})(1+5\hat{\lambda})}\pi\mu a^3\epsilon_{kmn}P_{2mj}E_{jn}^\infty(0) + \frac{12}{(1+3\hat{\lambda})^2}\pi\mu a^3 P_{2pk}(\Omega_p^\infty(0) - \Omega_p) \\
&\quad - \frac{8/7}{1+3\hat{\lambda}}\pi\mu a^5\epsilon_{klm}\left[-\nabla_j\nabla_p E_{pl}^\infty\big|_0 P_{2mj} + \nabla_j\nabla_l E_{mq}^\infty\big|_0 P_{2jq} + (1/2)\nabla^2 E_{mq}^\infty\big|_0 P_{2lq}\right], \qquad (4.10b) \\
\mathcal{L}_k^O &= -a(7/90)\langle\lambda S_{3pij}\rangle\int_{S_p} S_{3pij}\epsilon_{kln}x_l R_{mn}^{\parallel}(-p^\infty(0)n_m + x_q\nabla_q\sigma_{mr}^\infty(0)\, n_r + \cdots)\,\mathrm{d}S \\
&= -\frac{8/5}{(1+3\hat{\lambda})}\pi\mu a^4\epsilon_{kln}\nabla_q E_{mn}^\infty\big|_0 P_{3lmq}. \qquad (4.10c)
\end{aligned}$$

Note that the torque-strain coupling term $\epsilon_{kmn}P_{2mj}E_{jn}^\infty(0)$ comes from $\mathcal{L}_k^Q$ in (4.10*b*) due to the quadrupole. Combining (4.9) and (4.10) yields the extended Faxén relation for the torque:

$$\begin{aligned}
\mathcal{L}_k &= \frac{8}{1+3\hat{\lambda}}\pi\mu a^3\left[\delta_{pk} + \frac{3/2}{1+3\hat{\lambda}}P_{2pk}\right](\Omega_p^\infty(0) - \Omega_p) \\
&\quad - \frac{20}{(1+3\hat{\lambda})(1+5\hat{\lambda})}\pi\mu a^3\epsilon_{kmn}P_{2mj}E_{jn}^\infty(0) \\
&\quad - \frac{24/5}{1+3\hat{\lambda}}\pi\mu a^4\epsilon_{kmn}(\nabla_m E_{jn}^\infty\big|_0 P_{1j} - \nabla_p E_{pm}^\infty\big|_0 P_{1n})
\end{aligned}$$

$$-\frac{8/5}{(1+3\hat{\lambda})}\pi\mu a^4\epsilon_{kln}\nabla_q E^{\infty}_{mn}\big|_0 P_{3lmq}$$
$$-\frac{8/7}{1+3\hat{\lambda}}\pi\mu a^5\epsilon_{kln}\left[-\nabla_j\nabla_q E^{\infty}_{ql}\big|_0 P_{2nj}+\nabla_j\nabla_l E^{\infty}_{nq}\big|_0 P_{2jq}+(1/2)\nabla^2 E^{\infty}_{nq}\big|_0 P_{2ql}\right]. \tag{4.11}$$

Again, in a linear flow field or if (4.7) is satisfied, (4.11) is reduced to

$$\frac{\mathcal{L}_k}{\pi\mu a^3}=\frac{8}{1+3\hat{\lambda}}\left[\delta_{pk}+\frac{3/2}{1+3\hat{\lambda}}P_{2pk}\right](\Omega^{\infty}_p(0)-\Omega_p)-\frac{20}{(1+3\hat{\lambda})(1+5\hat{\lambda})}\epsilon_{kmn}P_{2mj}E^{\infty}_{jn}(0). \tag{4.12}$$

Equation (4.12) indicates that only a symmetric quadrupole contributes to the torque due to slip anisotropy. Antisymmetric dipoles and octupoles will enter to influence the torque if the imposed strain field is non-uniform, as revealed by (4.11). Note that the second term in (4.12) is the torque arising from torque-strain coupling, as illustrated in figure 4(*b*). The form of (4.12) also agrees with that found by Premlata & Wei (2021) who derived the coupled Faxén relations for the force and torque on a non-uniform slip sphere. It is worth mentioning that an additional torque can also be generated from the translational motion of a stick–slip sphere owing to unequal drag forces exerted on the stick and slip surfaces of the sphere. Such torque arises from torque-translation coupling and can only be realized through a dipole (Premlata & Wei 2021), different than that arising from torque-strain coupling in (4.12).

5. Rheology of a suspension of stick–slip spheres

Having determined the stresslet (4.8) for a stick–slip sphere, in this section we will put forth to examine its impacts on the rheology of a dilute suspension of force-free stick–slip spheres in a simple shear flow of shear rate $\dot{\gamma}$:

$$\boldsymbol{u}^{\infty}=-\dot{\gamma}x_2e_1,\quad \boldsymbol{E}^{\infty}=-(\dot{\gamma}/2)(e_2e_1+e_1e_2),\quad \text{and}\quad \boldsymbol{\Omega}^{\infty}=(\dot{\gamma}/2)e_3. \tag{5.1a–c}$$

Here we take the direction of the shear flow to be $-e_1$. This is to make the vorticity Ω^{∞} positive in e_3 in order to more conveniently analyse the features of a dipolar suspension in § 6 later. The presence of the spheres will cause an additional stress on the ambient fluid. If the suspension is homogeneous, this additional particle stress, which is reflected by the stresslet (4.8), affecting the average bulk stress of the suspension according to (Batchelor 1970)

$$\langle\Sigma_{ij}\rangle=-\langle p\rangle\delta_{ij}+2\mu\langle e_{ij}\rangle+n\langle\mathcal{S}_{ij}\rangle, \tag{5.2}$$

where $n=\phi/V_p$ is the number density of the spheres in terms of the ratio of the volume fraction ϕ to the sphere's volume $V_p=4\pi a^3/3$. In simple shear flow, the average rate of strain $\langle e_{ij}\rangle=E^{\infty}_{ij}$.

Given that the stresslet (4.8) is anisotropic depending on the sphere's orientation, to find the average stresslet $\langle\mathcal{S}_{ij}\rangle$ for determining the average bulk stress $\langle\Sigma_{ij}\rangle$ given by (5.2), it is necessary to express the stresslet in terms of the sphere's stick–slip director $\boldsymbol{d}$ (defined in the direction from the stick face to the slip face, see § 3). This is done by converting $\boldsymbol{P}_2$ and $\boldsymbol{P}_4$ in (4.8) into $\boldsymbol{d}$ using (3.10*b*) and (3.10*d*). It is also more convenient to express $\boldsymbol{d}=(d_1,d_2,d_3)$ using spherical polar coordinates in terms of polar angle θ and azimuthal

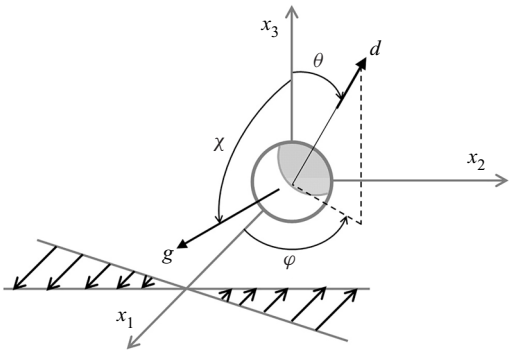

Figure 5. The spherical polar coordinates for describing the orientational dynamics of a stick–slip Janus sphere in a simple shear flow. The sphere can become dipolar to possess a couple in an external force field $\boldsymbol{g}$ when it has a permanent dipole moment along the stick–slip director $\boldsymbol{d}$.

angle φ (see figure 5):

$$d_1 = \sin\theta\cos\varphi, \quad d_2 = \sin\theta\sin\varphi \quad \text{and} \quad d_3 = \cos\theta. \tag{5.3a–c}$$

With the above, (4.8) can be rewritten as

$$\frac{\mathcal{S}_{ij}}{(4/3)\pi\mu a^3} = 5\left(\frac{1+2\hat{\lambda}}{1+5\hat{\lambda}}\right)E^{\infty}_{ij}(0) + \Bigg[c_1 E^{\infty}_{ij}(0) + c_2(d_i d_j - \frac{1}{3}\delta_{ij})d_l d_k E^{\infty}_{lk}(0) + c_3(d_i d_k E^{\infty}_{jk}(0) + d_j d_k E^{\infty}_{ik}(0) - \frac{2}{3}\delta_{ij}d_l d_k E^{\infty}_{lk}(0)) + c_4\left(d_j\epsilon_{ilk}d_k + d_i\epsilon_{jlk}d_k\right)(\Omega^{\infty}_l(0) - \Omega_l)\Bigg], \tag{5.4}$$

wherein the $O(\varepsilon)$ coefficients in the anisotropic part can be expressed in terms of the quadrupole strength $\mathcal{Q}$ and the hexadecapole strength $\mathcal{H}$:

$$\left.\begin{aligned} c_1 &= \frac{5}{7}\frac{(15\mathcal{Q}+8\mathcal{H})}{(1+5\hat{\lambda})^2}, \quad c_2 = \frac{100\mathcal{H}}{(1+5\hat{\lambda})^2}, \\ c_3 &= -\frac{25}{7}\frac{((9/2)\mathcal{Q}+8\mathcal{H})}{(1+5\hat{\lambda})^2}, \quad c_4 = -\frac{(45/2)\mathcal{Q}}{(1+3\hat{\lambda})(1+5\hat{\lambda})}. \end{aligned}\right\} \tag{5.5}$$

Note that the c_4 rotational contribution is reflected solely by quadrupole, as will also be seen in the orientational dynamics of the sphere in § 6.1.

Recall that for a given stick–slip geometry, the strengths of surface moments can be related to the coefficients of the Legendre series for the slip distribution (see (3.13)). This will allow us to determine (5.5) for a given stick–slip pattern. For instance, for a two-faced stick–slip Janus sphere (see figure 3), (5.5) can be re-expressed as follows by replacing $\mathcal{H}$

and $\mathcal{Q}$ using (3.14*c*,*e*):

$$\left.\begin{aligned} c_1 &= \frac{5}{14}\left((9/2)+7\cos^2\alpha\right)\frac{(\lambda^+-\lambda^-)\sin^2\alpha\cos\alpha}{(1+5\hat{\lambda})^2},\\ c_2 &= \frac{25}{4}\left(7\cos^2\alpha-3\right)\frac{(\lambda^+-\lambda^-)\sin^2\alpha\cos\alpha}{(1+5\hat{\lambda})^2},\\ c_3 &= -\frac{25}{14}\left(7\cos^2\alpha-(3/4)\right)\frac{(\lambda^+-\lambda^-)\sin^2\alpha\cos\alpha}{(1+5\hat{\lambda})^2},\\ c_4 &= -\frac{45}{8}\frac{(\lambda^+-\lambda^-)\sin^2\alpha\cos\alpha}{(1+3\hat{\lambda})(1+5\hat{\lambda})}, \end{aligned}\right\} \tag{5.6}$$

where $\hat{\lambda}=\langle\lambda\rangle$ is given by (3.14*a*) and also varies with λ^+, λ^- and α. Equation (5.6) provides direct links between the strengths of various stresslet contributions in (5.4) and the stick–slip partition, which will be useful when coming to compute the average bulk properties of a suspension of stick–slip Janus spheres.

Consider that the stick–slip spheres are couple-free, so the last term due to their rotations in (5.4) has no contribution (up to $O(\varepsilon)$ since $(\Omega_l^\infty(0)-\Omega_l)=O(\varepsilon)$ according to (4.12)). Since the directors of these spheres can still vary stochastically, the average of a property $\mathcal{M}$ of a suspension of stick–slip spheres can be obtained from its angle average,

$$\langle\mathcal{M}(\theta,\varphi)\rangle=\int_0^{\pi}\int_0^{2\pi}\sin\theta\,\mathcal{M}(\theta,\varphi)\Psi(\theta,\varphi)\,\mathrm{d}\varphi\,\mathrm{d}\theta, \tag{5.7}$$

weighted with the orientation probability distribution function Ψ for the director $\boldsymbol{d}$, in contrast to Ramachandran & Khair (2009) who treated all the spheres as orienting in the same direction. Because slip anisotropy is assumed weak here, hydrodynamically a weakly stick–slip sphere may behave like a no-slip near sphere. There are two reasons for this analogy. First, geometrically the shape of a near sphere can also be represented by surface spherical harmonics (Brenner 1964), just like (3.4) for the slip distribution of a stick–slip sphere. Second, when taking a small asphericity expansion for the no-slip boundary condition applied on the surface of a near sphere, the resulting expression at first order resembles the slip boundary condition (2.6*b*) whose slip length is varying with the shape of the near sphere.

Having the above analogy in mind, we next show how to make use of the orientation probability distribution Ψ for a near sphere to determine that for a weakly stick–slip sphere. Hinch & Leal (1972) showed that the former is controlled by the Bretherton parameter $\mathcal{B}$ arising from small asphericity (Bretherton 1962),

$$\Psi(\theta,\varphi)=\frac{1}{4\pi}\left[1+\mathcal{B}\,\frac{3\sin^2\theta\,\sin(2\varphi-\tan^{-1}(\dot{\gamma}/6D_r))}{2(1+(6D_r/\dot{\gamma})^2)^{1/2}}\right], \tag{5.8}$$

with a modulation by the ratio of shear rate $\dot{\gamma}$ to the rotary diffusion coefficient D_r of the sphere. For a weakly stick–slip sphere considered here, its asphericity is caused by small slip anisotropy, allowing its orientation behaviour to be also controlled by the Bretherton parameter $\mathcal{B}=O(\varepsilon)$ in the same manner as (5.8). As will be shown later in § 6.1, the value of $\mathcal{B}$ is found to be proportional to the strength $\mathcal{Q}$ of quadrupole, determined from the angular velocity and the equation governing the orientational dynamics (up to $O(\varepsilon)$)

of the sphere (see (6.4) and (6.5)). That is,

$$\dot{d}_i = \epsilon_{ijk}\Omega_j d_k = \epsilon_{ijk}\Omega_j^{\infty} d_k + \mathcal{B}(\delta_{ij} - d_i d_j)E_{jk}^{\infty} d_k, \tag{5.9a}$$

$$\mathcal{B} = -\frac{(15/2)\mathcal{Q}}{1+5\hat{\lambda}}. \tag{5.9b}$$

Equation (5.9*a*) is also exactly the equation governing the orientational dynamics of an axisymmetric spheroid (Kim & Karrila 1991). Therefore, a symmetric stick–slip sphere can be made analogous to a spheroid by relating their shape factors through (5.9*b*). A stick–slip–stick (slip–stick–slip) sphere with $\mathcal{Q} < 0$ ($\mathcal{Q} > 0$) acts like a prolate (oblate) spheroid with $\mathcal{B} > 0$ ($\mathcal{B} < 0$). Such a spheroid with small $\mathcal{B}$ is a special class of near spheres, allowing us to use (5.9*b*) in (5.8) for determining Ψ for a weakly stick–slip sphere.

Using (5.7), (5.8) and (5.9*b*), we can evaluate each component of $\langle \Sigma_{ij} \rangle$ in (5.2) according to

$$\langle \Sigma_{12} \rangle = \mu\dot{\gamma} + \phi\mu\ \dot{\gamma}\left[\frac{5}{2}\left(\frac{1+2\hat{\lambda}}{1+3\hat{\lambda}}\right) + \frac{1}{2}\left\langle c_1 + 2c_2\ d_1^2 d_2^2 + c_3\ (d_1^2 + d_2^2)\right\rangle\right], \tag{5.10a}$$

$$\langle \Sigma_{11} \rangle = \langle p \rangle + \phi\mu\dot{\gamma}\ (1/3)\ \left\langle d_1 d_2\left[c_2\ (3d_1^2 - 1) + c_3\right]\right\rangle, \tag{5.10b}$$

$$\langle \Sigma_{22} \rangle = \langle p \rangle + \phi\mu\dot{\gamma}\ (1/3)\ \left\langle d_1 d_2\left[c_2\ (3d_2^2 - 1) + c_3\right]\right\rangle, \tag{5.10c}$$

$$\langle \Sigma_{33} \rangle = \langle p \rangle + \phi\mu\dot{\gamma}\ (1/3)\ \left\langle d_1 d_2\left[c_2\ (3d_3^2 - 1) - 2c_3\right]\right\rangle. \tag{5.10d}$$

The average shear stress $\langle \Sigma_{12} \rangle$ provides the measure for the Einstein effective viscosity $\mu_{eff}^{(E)} = \mu(1 + \langle \Sigma_{12} \rangle/\dot{\gamma})$ from (5.10*a*). We find that in the evaluation of $\langle \Sigma_{12} \rangle$, the contribution from the angle-dependent $\mathcal{B}$ term due to slip anisotropy in the orientation distribution function (5.8) is identically zero. The resulting effective viscosity is found to be

$$\mu_{eff}^{(E)} = \mu\left[1 + \phi\left(\frac{5}{2}\left(\frac{1+2\hat{\lambda}}{1+5\hat{\lambda}}\right) + \frac{1}{2}\left(c_1 + \frac{2}{15}c_2 + \frac{2}{3}c_3\right)\right)\right]. \tag{5.11}$$

Equation (5.11) indicates that slip anisotropy will not only contribute an $O(\phi\varepsilon)$ correction to the effective viscosity but also the correction will be independent of shear rate $\dot{\gamma}$. This is very different from the effective viscosity of a suspension of near spheres (Hinch & Leal 1972) in that the viscosity correction due to small asphericity of amplitude $a\varepsilon$ is $O(\phi\varepsilon^2)$ and shear-rate dependent. In addition, such slip anisotropy correction to the effective viscosity can be either positive or negative, depending on the values of c_1, c_2 and c_3 from the stick–slip pattern. If the spheres are of stick–slip–stick or slip–stick–slip type represented by a quadrupole without a hexadecapole, in particular, $c_2 = 0$ and $c_1 + (2/3)c_3 = 0$ result in no correction at $O(\phi\varepsilon)$, meaning that in this case the slip-anisotropy correction to the effective viscosity will start at $O(\phi\varepsilon^2)$.

Figure 6 plots the behaviour of the effective viscosity (5.11) of a dilute couple-free suspension of two-faced stick–slip spheres. Here we plot the $O(\phi)$ correction as a function of the stick–slip division angle α for different values of the stick–slip contrast $(\lambda^+ - \lambda^-)$ (with $\lambda^- = 0$ here). It is clear that the results are lower than the value 2.5 of the Einstein viscosity but higher than the value 1.5 corresponding to the bubble limit. For a given value of $(\lambda^+ - \lambda^-)$, the viscosity is decreased as the slip portion is increased with α, which is expected.

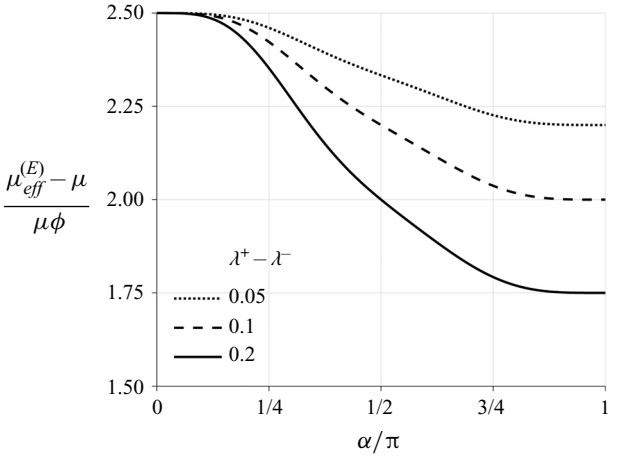

Figure 6. Plot of the $O(\phi)$ correction to the effective viscosity of a dilute couple-free suspension of two-faced stick–slip spheres as a function of the stick–slip division angle α. Results are plotted for different values of the stick–slip contrast $(\lambda^+ - \lambda^-)$ (with $\lambda^- = 0$ here), showing lower than the value 2.5 of the Einstein viscosity but higher the value 1.5 corresponding to the bubble limit. For a given value of $(\lambda^+ - \lambda^-)$, the viscosity is decreased as the slip portion is increased with α.

The diagonal components of the bulk stress allow us to determine the first and second normal stress differences, $N_1 = \Sigma_{11} - \Sigma_{22}$ and $N_2 = \Sigma_{22} - \Sigma_{33}$. Since these components are $O(\phi\varepsilon)$ from the anisotropic part of the stresslet (5.4) and non-zero average contributions to them come only from the $O(\varepsilon)$ angle-dependent part of the orientation probability distribution (5.8) (because $\mathcal{B} = O(\varepsilon)$), the average normal stress differences $\langle N_1 \rangle$ and $\langle N_2 \rangle$ generally start at $O(\phi\varepsilon^2)$. The actual calculations yield

$$\langle N_1 \rangle = 0, \tag{5.12a}$$

$$\langle N_2 \rangle = \mu\dot{\gamma}\phi\frac{\mathcal{B}}{4}\left(\frac{c_2}{5} + c_3\right)\left[\frac{\dot{\gamma}/6D_r}{1 + (\dot{\gamma}/6D_r)^2}\right]. \tag{5.12b}$$

It turns out that a non-zero contribution to $\langle N_1 \rangle$ will start at $O(\phi\varepsilon^3)$, which differs from the result of Hinch & Leal (1972) for a near-sphere suspension; $\langle N_2 \rangle$ is $O(\phi\varepsilon^2)$, as expected. Note that the Bretherton parameter $\mathcal{B} \propto -\mathcal{Q}$ in (5.12*b*) is determined solely by a quadrupole in view of (5.9*b*) and thus acts like c_4. Equation (5.12*b*) reveals that if the sphere's surface is constituted purely by a quadrupole, $c_2 = 0$ and $c_3 \propto -\mathcal{Q}$ will make $\langle N_2 \rangle \propto \mathcal{Q}^2$ always positive, regardless of whether the sphere is of slip–stick–slip ($\mathcal{Q} > 0$) or stick–slip–stick ($\mathcal{Q} < 0$) type. In fact, for a two-faced stick–slip sphere, it can be shown using (5.6) that even including hexadecapole contributions with $\mathcal{H} \neq 0$ still leads $\langle N_2 \rangle$ described by (5.12*b*) to be always non-negative. Furthermore, $\langle N_2 \rangle \propto \dot{\gamma}^2$ in the weak shear $\dot{\gamma} \to 0$ limit, but turns to approach a constant in the strong shear $\dot{\gamma} \to \infty$ limit. This behaviour can be clearly seen in figure 7(*a*) that plots $\langle N_2 \rangle$ as a function of $\dot{\gamma}$ for a suspension of two-faced stick–slip spheres. Such rate-dependent behaviour for $\langle N_2 \rangle$ also agrees with that found by Hinch & Leal (1972) for a near-sphere suspension.

In terms of impacts of stick–slip geometry, figure 7(*b*) plots how $\langle N_2 \rangle$ varies with the stick–slip contrast $(\lambda^+ - \lambda^-)$ and the stick–slip division angle α for a suspension of two-faced stick–slip spheres. First of all, we find that $\langle N_2 \rangle \geq 0$, which can be proved from (5.12*b*) using (5.6). Second, the amplitude of $\langle N_2 \rangle$ is increased with $(\lambda^+ - \lambda^-)$. In fact, it can be shown that $\langle N_2 \rangle \propto (\lambda^+ - \lambda^-)^2$ according to (5.12*b*) and (5.6). Interestingly, how

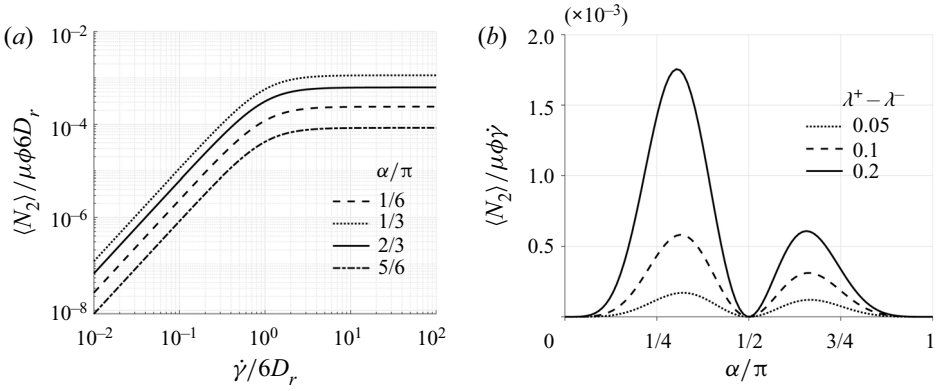

Figure 7. Behaviours of the average second normal stress difference $\langle N_2\rangle$ described by (5.12*b*) for a suspension of two-faced stick–slip spheres. (*a*) Plot of $\langle N_2\rangle$ against shear rate $\dot{\gamma}/6D_r$ for different values of the stick–slip division angle α; $(\lambda^+ - \lambda^-) = 0.1$. (*b*) Plot of $\langle N_2\rangle$ against the stick–slip division angle α for different values of the stick–slip contrast $(\lambda^+ - \lambda^-)$. $\dot{\gamma}/6D_r = 1$. Note that if the spheres are precisely half-faced with an antisymmetric dipole only, $\langle N_2\rangle = 0$.

$\langle N_2\rangle$ varies with α is not monotonic – it varies up and down as increasing the slip portion. In particular, the maximum value of $\langle N_2\rangle$ occurs to the spheres having more stick portions ($\alpha < \pi/2$) and located at a particular value of α, depending on $(\lambda^+ - \lambda^-)$. For instance, for $(\lambda^+ - \lambda^-) = 0.2$, the maximum of $\langle N_2\rangle$ occurs at around $\alpha = \pi/4$ but shifts to a higher value as $(\lambda^+ - \lambda^-)$ is decreased. Also recall from (5.12*b*) that only quadrupoles and hexadecapoles contribute to $\langle N_2\rangle$. If the spheres are precisely half-faced ($\alpha = \pi/2$), $\langle N_2\rangle = 0$ since the slip pattern is described solely by an antisymmetric dipole without a symmetric quadrupole and hexadecapole, as also displayed in the figure.

As shown above, the average bulk properties of a suspension of weakly stick–slip spheres behave quite differently compared with those of a suspension of no-slip near spheres found by Hinch & Leal (1972). The differences in rheology between these two suspensions is attributed to the fact that slip anisotropy is not just geometric asymmetry. The reason is that the strain resistance matrix (4.1*a*) has an additional contribution $\boldsymbol{nnn}$ when $\hat{\lambda} \neq 0$. Physically, this contribution comes from the double-layer part of the boundary integral representation of the Stokes flow field solution. Such a contribution vanishes for a no-slip particle. However, if there is slip on the surface of a particle, this double-layer contribution can cause an additional pressure gradient through the non-vanishing slip velocity on the particle's surface. To form a symmetric force dipole, namely stresslet, for a stick–slip particle in a linear flow field through this slip-induced pressure gradient, it is determined not only by the slip asymmetry but also by how the particle orients with respect to the flow field since the pressure will join with the stick–slip pattern to affect the local force distribution which generally is not symmetric. For a no-slip particle, on the contrary, an anisotropy in the stresslet only requires an asymmetry in geometry because it is determined purely by the deviatoric part of the stress tensor without pressure.

6. Stick–slip sphere with couple: non-Jeffery orbits and spin-induced stresslet

6.1. *Non-Jeffery orbits*

The results presented in the preceding section are based on the couple-free situation under which there is no net torque on a force-free stick–slip sphere. However, if the sphere

possesses a permanent dipole and spins due to an external couple, an additional stresslet can arise from such dipolar spinning, as indicated by (5.4). This will alter not only the orientational dynamics of a stick–slip sphere, but also the suspension rheology. Since the average behaviour of the stresslet in the latter will depend crucially on the orientation of the sphere in the former that may display a preferential direction, in this section we will look at how a stick–slip sphere behaves in its orientational dynamics with and without an external couple.

Suppose that a stick–slip sphere possesses a permanent dipole moment if there exists an inhomogeneity in the internal mass distribution or a permanent magnetic/electric dipole embedded within the sphere (Brenner 1970). In our case, we assume that such a permanent dipole acts along the direction of the stick–slip director $\boldsymbol{d}$ and takes the form $(4\pi/3)\rho a^3\boldsymbol{d}$ with ρ being the density of the sphere. This can likely be the case since a polarity may be naturally brought out by the stick–slip asymmetry through the distinct material properties of the stick and the slip faces. When an external force field $\boldsymbol{g}$ is applied, if such dipole is not aligned to $\boldsymbol{g}$, a body couple $\mathcal{L}_k^{(e)}$ will be generated to exert on the sphere according to (Brenner 1970)

$$\mathcal{L}_k^{(e)} = \frac{4\pi}{3}\rho a^3 \boldsymbol{d}\times\boldsymbol{g}. \tag{6.1}$$

Consider such a dipolar stick–slip sphere freely suspending in a simple shear flow (5.1*a–c*). Then the applied external torque (6.1) has to be balanced by the hydrodynamic torque $\mathcal{L}_k$ given by (4.12): $\mathcal{L}_k + \mathcal{L}_k^{(e)} = 0$. We determine the sphere's angular velocity $\boldsymbol{\Omega}$ in a perturbative manner by taking small ε expansions below for both Ω_k and $\mathcal{L}_k$ followed by their substitutions into the above zero-net-torque condition:

$$\Omega_k = \Omega_k^{(0)} + \Omega_k^{(1)} + \cdots, \tag{6.2a}$$

$$\mathcal{L}_k = \mathcal{L}_k^{(0)} + \mathcal{L}_k^{(1)} + \cdots. \tag{6.2b}$$

At $O(\varepsilon^0)$

$$\mathcal{L}_k^{(0)} + \mathcal{L}_k^{(e)} = 0, \tag{6.3a}$$

with $\mathcal{L}_k^{(0)}$ given by (4.9), (6.3*a*) yields the leading-order rate of rotation

$$\Omega_k^{\infty}(0) - \Omega_k^{(0)} = -(1+3\hat{\lambda})\Omega_k^d, \tag{6.3b}$$

to be equal to the angular velocity due to the permanent dipole

$$\boldsymbol{\Omega}^d = \beta\dot{\gamma}\boldsymbol{d}\times\hat{\boldsymbol{g}}, \tag{6.3c}$$

where

$$\beta = \rho g/3\mu\dot{\gamma} \tag{6.3d}$$

is the dimensionless parameter measuring the magnitude of the dipole-induced angular velocity relative to the flow vorticity of $\dot{\gamma}/2$, and $\hat{\boldsymbol{g}} = \boldsymbol{g}/g = \boldsymbol{e}_1\sin\chi + \boldsymbol{e}_3\cos\chi$ is the direction of the external force acting in an angle χ with respect to the direction of the flow vorticity (see figure 5).

At $O(\varepsilon)$

$$\mathcal{L}_k^{(1)} = -\Omega_k^{(1)} - \frac{3}{2}P_{2kp}\Omega_p^d - \frac{5/2}{1+5\hat{\lambda}}\epsilon_{kmn}P_{2mj}E_{jn}^{\infty}(0) = 0, \tag{6.3e}$$

which yields

$$\Omega_k^{(1)} = -\frac{3}{2}P_{2kp}\Omega_p^d - \frac{5/2}{1+5\hat{\lambda}}\epsilon_{kmn}P_{2mj}E_{jn}^{\infty}(0). \tag{6.3f}$$

Combining (6.3*b*) and (6.3*f*), the rate of rotation for the sphere can be determined as

$$\Omega_k^{\infty}(0) - \Omega_k = -(1+3\hat{\lambda})\Omega_k^d + \frac{3}{2}P_{2pk}\Omega_p^d + \frac{5/2}{1+5\hat{\lambda}}\epsilon_{kmn}P_{2mj}E_{jn}^{\infty}(0). \tag{6.4}$$

Using (6.4) together with (3.10*b*) for P_{2ij}, the orientational dynamics of the sphere is governed by the following equation in terms of the director $\boldsymbol{d}$:

$$\begin{aligned}\dot{\boldsymbol{d}} &= \boldsymbol{\Omega}\times\boldsymbol{d}\\ &= \boldsymbol{\Omega}^{\infty}(0)\times\boldsymbol{d} + \beta(1+3\hat{\lambda})\hat{\boldsymbol{g}}\left[1-\frac{\mathcal{B}}{5}\left(\frac{1+5\hat{\lambda}}{1+3\hat{\lambda}}\right)\right]\cdot(\boldsymbol{I}-\boldsymbol{dd}) + \mathcal{B}\boldsymbol{E}^{\infty}\cdot\boldsymbol{d}\cdot(\boldsymbol{I}-\boldsymbol{dd}).\end{aligned} \tag{6.5}$$

Equation (6.5) with $\mathcal{B}=0$ recovers the equation governing the orientational dynamics of a homogenous dipolar sphere (Brenner 1970). For a stick–slip sphere without a permanent dipole at $\beta=0$, (6.5) is reduced to (5.9*a*) with the Bretherton parameter $\mathcal{B}$ given by (5.9*b*). When there is a permanent dipole, not only an additional spinning due to the β term emerges to affect the orientation of the sphere, but also such dipolar spinning is modified by slip anisotropy through $\mathcal{B}$.

Making use of (5.3*a–c*) together with the following identities (Kim & Karrila 1991)

$$\dot{d}_3 = -\sin\theta\dot{\theta} \quad \text{and} \quad d_1\dot{d}_2 - d_2\dot{d}_1 = \sin^2\theta\dot{\varphi}, \tag{6.6a,b}$$

we can rewrite (6.5) in terms of spherical polar coordinates, allowing us to examine the director trajectory of a stick–slip sphere under the actions of both the imposed flow field (5.1*a–c*) and the external force field $\boldsymbol{g}$:

$$\dot{\theta} = \beta(1+3\hat{\lambda})\left[1-\frac{\mathcal{B}}{5}\left(\frac{1+5\hat{\lambda}}{1+3\hat{\lambda}}\right)\right](\cos\theta\cos\varphi\sin\chi - \sin\theta\cos\chi) - \frac{\dot{\gamma}}{4}\mathcal{B}\sin 2\theta\sin 2\varphi, \tag{6.7a}$$

$$\dot{\varphi} = \frac{\dot{\gamma}}{2} - \beta(1+3\hat{\lambda})\left[1-\frac{\mathcal{B}}{5}\left(\frac{1+5\hat{\lambda}}{1+3\hat{\lambda}}\right)\right]\csc\theta\sin\varphi\sin\chi - \frac{\dot{\gamma}}{2}\mathcal{B}(\cos^2\varphi - \sin^2\varphi). \tag{6.7b}$$

Equation (6.7) with $\mathcal{B}=0$ recovers the equations obtained previously by Hall & Busenberg (1969) for a homogenous dipolar sphere. Figure 8(*a*) plots the director trajectory for a two-faced stick–slip sphere without dipolar spinning when $\beta=0$, showing a closed Jeffery orbit like that of an axisymmetric spheroid. When the sphere undergoes dipolar spinning, figure 8(*b–d*) display the director trajectories of the sphere with different values of β, showing that the sphere with a given value of β typically will eventually end up with a fixed orientation, much like the orientation behaviour of a dipolar uniform-slip

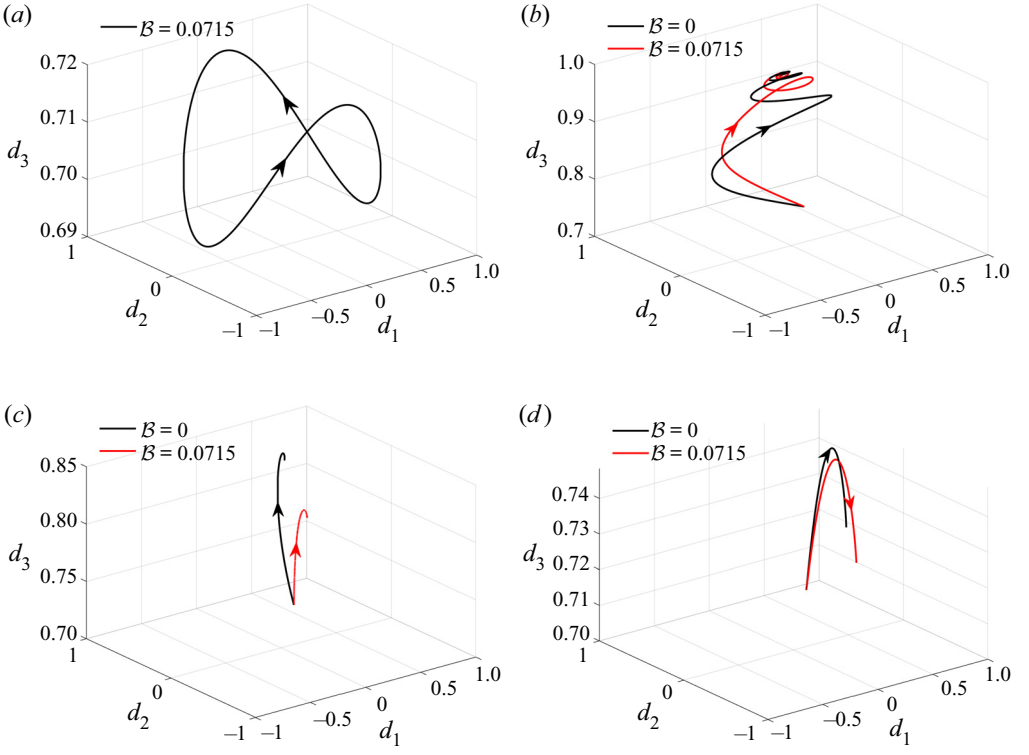

Figure 8. Computed director trajectories of a two-faced stick–slip sphere with $\mathcal{B} = 0.0715$ (from $\mathcal{Q}$ in (3.14*c*) and (5.9*b*) with $\lambda^+ - \lambda^- = 0.2$, $\lambda^- = 0$, and $\alpha = 3\pi/4$) in a simple shear flow. Panel (*a*) plots the case without dipolar spinning ($\beta = 0$), showing a typical closed Jeffery orbit. Panels (*b–d*) are the results at different values of β when the sphere undergoes a dipolar spinning with $\chi = \pi/4$: (*b*) $\beta = 0.1$; (*c*) $\beta = 0.5$; (*d*) $\beta = 1.5$. In this case, for a given value of β the sphere typically will end up with a fixed orientation, much like the behaviour of a dipolar uniform-slip sphere with $\mathcal{B} = 0$. In all cases, the initial orientation angles $(\theta, \varphi) = (\pi/4, \pi/4)$ and the data are collected at time to $t = 150\dot{\gamma}^{-1}$.

sphere with $\mathcal{B} = 0$ (Brenner 1970). Displaying a fixed orientation for a dipolar sphere with and without slip anisotropy is essentially the result that the dipolar spinning is balanced by the flow vorticity. As will be shown shortly in § 6.2, this result will significantly affect the rheology of a suspension of stick–slip spheres since every sphere in the suspension possess the same stresslet provided that rotary Brownian motion is negligible. In this case, the impacts of slip anisotropy on the stresslet will occur at $O(\varepsilon)$ due to the ***dd*** and ***dddd*** terms, just like those shown in (5.4). The corresponding correction to the bulk stress will therefore be $O(\phi\varepsilon)$.

For the special case of $\chi = \pi/2$ and $\beta < 1$, Hall & Busenberg (1969) showed for a homogeneous sphere that instead of tending in time to a fixed orientation, it will undergo a periodic precession, signified by a closed orbit in its orientational dynamics. This is illustrated by the computed orientation trajectory for a dipolar slip sphere, as shown in figure 9. For a dipolar stick–slip sphere under the same condition, its director trajectory is pretty much like the above with a slight change due to slip anisotropy, as also shown in figure 9.

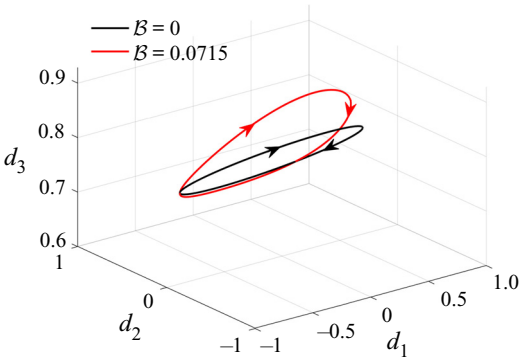

Figure 9. Computed director trajectory of a dipolar stick–slip sphere for the special case of $\chi = \pi/2$ and $\beta < 1$. The result is obtained at $\beta = 0.1$ and $\mathcal{B} = 0.0715$ (from $\mathcal{Q}$ in (3.14*c*) and (5.9*b*) with $\lambda^+ - \lambda^- = 0.2$, $\lambda^- = 0$ and $\alpha = 3\pi/4$), displaying a closed orbit that signifies a periodic precession, similar to the result for a uniform-slip sphere with $\mathcal{B} = 0$. The calculations are performed with the initial orientation angles $(\theta, \varphi) = (\pi/4, \pi/4)$ and the data are collected at time to $t = 150\dot{\gamma}^{-1}$.

6.2. *Additional bulk stress induced by dipolar spinning*

As shown above, a stick–slip sphere possessing a persistent dipolar spin typically displays a fixed orientation in a simple shear flow. The bulk stress of a suspension of such dipolar stick–slip spheres is expected to behave differently compared with the features shown in § 5 under the couple-free condition, which will be demonstrated in this subsection.

According to Batchelor (1970), for a homogeneous particle suspension, the excess bulk stress $\Sigma_{ij}^{(p)}$ due to the presence of particles generally consists of two contributions: the symmetric contribution from stresslet $\mathcal{S}_{ij}$; and the antisymmetric contribution from couplet $(1/2)\epsilon_{ijk}\mathcal{L}_k$,

$$\Sigma_{ij}^{(p)} = n\mathcal{S}_{ij} + n(1/2)\epsilon_{ijk}\mathcal{L}_k. \tag{6.8}$$

The antisymmetric stress due to a couplet can arise when a particle possesses a persistent spin due to an externally imposed couple $-\mathcal{L}_k$, as shown by Brenner (1970) for a dilute suspension of dipolar spherical particles. It should be noted that the symmetric stress due to $\mathcal{S}_{ij}$ also involves the rotational contribution from $\mathcal{L}_k$ proportional to the rate of rotation $(\Omega_k^\infty - \Omega_k)$ for an anisotropic particle, as seen from (3.1). For a suspension of dipolar stick–slip spheres, apart from the bulk stress due to the imposed strain field E_{ij}^∞, the rotational part in (3.1) and the couplet contribution in (6.8) combined are responsible for the additional bulk stress $\Sigma_{ij}^{(d)}$ due to the dipolar spinning of these heterogeneous spheres. As such, this spin-induced stress also comprises both symmetric and antisymmetric contributions:

$$\Sigma_{ij}^{(d)} = \Sigma_{ij}^{(d)S} + \Sigma_{ij}^{(d)A}. \tag{6.9}$$

The symmetric part comes from the c_4 term of $O(\varepsilon)$ in (5.4) with the rate of rotation given by (6.4):

$$\begin{aligned}\Sigma_{ij}^{(d)S} &= \phi\mu c_4 \left(d_j\epsilon_{ilk}d_k + d_i\epsilon_{jlk}d_k\right)(\Omega_l^\infty(0) - \Omega_l) \\ &= -\phi\mu(1 + 3\hat{\lambda})c_4(d_j\epsilon_{ilk} + d_i\epsilon_{jlk})\Omega_l^d d_k.\end{aligned} \tag{6.10}$$

In the above, we omit the strain field contribution from the last term in (6.4) since it contributes to $O(\phi\varepsilon^2)$ and hence is negligible. We also omit the quadrupole correction to

the sphere's angular velocity in (6.4) because of the same reason. The antisymmetric part comes from the $\mathcal{L}_k$ term in (6.9) and can be evaluated using (4.12) and (6.4):

$$\begin{aligned}\Sigma_{ij}^{(d)A} &= (3/8)\mu\phi\epsilon_{ijk}(\mathcal{L}_k/\pi\mu a^3)\\ &= -3\mu\phi\epsilon_{ijk}\Omega_k^d.\end{aligned} \tag{6.11}$$

This is exactly the bulk stress resulting directly from the external torque (6.1), i.e. $\mathcal{L}_k = -\mathcal{L}_k^{(e)}$ in the first line of (6.11), as given by Brenner (1970). This antisymmetric couplet stress contributes to the bulk stress at $O(\phi)$ and hence is more important than the symmetric stress (6.10) of $O(\varepsilon\phi)$.

Recall in § 6.1 that if rotary Brownian diffusion is negligible, all the dipolar spheres generally display the same orientation in a simple shear flow. Hence the average bulk stress should be represented by the bulk stress at that particular orientation $\boldsymbol{d} = \boldsymbol{d}_s$. The effective viscosity and normal stress differences should also be evaluated in the same manner with the corresponding orientation angles $(\theta, \varphi) = (\theta_s, \varphi_s)$ (Brenner 1970). We remark that in the previous study by Ramachandran & Khair (2009), stick–slip spheres were couple-free but still treated as oriented in the same direction in their calculations for the average rheology properties, which conflicts with the notion above.

Combining (6.10) and (6.11), each component of $\Sigma_{ij}^{(d)}$ in (6.9) can be determined as

$$\Sigma_{12}^{(d)} = \phi\mu\beta\dot{\gamma}[3d_2\sin\chi + c_4(1+3\hat{\lambda})d_2((d_1^2 - d_2^2 - d_3^2)\sin\chi + 2d_1d_3\cos\chi)], \tag{6.12a}$$

$$\Sigma_{11}^{(d)} = -2\phi\mu\beta\dot{\gamma}c_4(1+3\hat{\lambda})d_1[(d_2^2 + d_3^2)\sin\chi - d_1d_3\cos\chi], \tag{6.12b}$$

$$\Sigma_{22}^{(d)} = 2\phi\mu\beta\dot{\gamma}\ c_4(1+3\hat{\lambda})d_2^2\,[d_1\sin\chi + d_3\cos\chi]\,, \tag{6.12c}$$

$$\Sigma_{33}^{(d)} = 2\phi\mu\beta\dot{\gamma}\ c_4(1+3\hat{\lambda})d_3[d_1d_3\sin\chi - (d_1^2 + d_2^2)\cos\chi]. \tag{6.12d}$$

The corresponding effective viscosity is found to be

$$\begin{aligned}\frac{\mu_{eff}^{(d)}}{\mu\beta\phi} &= 3\sin\theta\sin\varphi\sin\chi + c_4(1+3\hat{\lambda})\sin\theta(\sin\varphi(2\sin^2\theta\cos^2\varphi - 1)\sin\chi\\ &\quad + \tfrac{1}{2}\sin 2\theta\sin 2\varphi\cos\chi).\end{aligned} \tag{6.13}$$

The first term comes from the antisymmetric stress (6.11), in accordance with the result obtained by Brenner (1970). The second term is from the symmetric stress (6.10), providing the slip anisotropy correction due to the quadrupole because $c_4 \propto -\mathcal{Q}$. If the sphere is half-faced (with dipole only), there will be no contribution to the correction term.

We also determine the first and second normal stress differences due to dipolar spinning, $N_1^{(d)} = \Sigma_{11}^{(d)} - \Sigma_{22}^{(d)}$ and $N_2^{(d)} = \Sigma_{22}^{(d)} - \Sigma_{33}^{(d)}$ as

$$N_1^{(d)} = 2\phi\mu\dot{\gamma}\beta c_4(1+3\hat{\lambda})\sin\theta[\cos\varphi(\sin^2\theta\cos 2\varphi - 1)\sin\chi + \tfrac{1}{2}\sin 2\theta\cos 2\varphi\cos\chi], \tag{6.14a}$$

$$\begin{aligned}N_2^{(d)} &= 2\phi\mu\dot{\gamma}\ \beta c_4(1+3\hat{\lambda})\sin\theta[\cos\varphi(\sin^2\theta\sin^2\varphi - \cos^2\theta)\sin\chi\\ &\quad + \frac{1}{2}\sin 2\theta(1+\sin^2\varphi)\cos\chi].\end{aligned} \tag{6.14b}$$

These stresses are $O(\phi\varepsilon)$ due again to quadrupole from the symmetric stress (6.10). They will vanish if the sphere is half-faced.

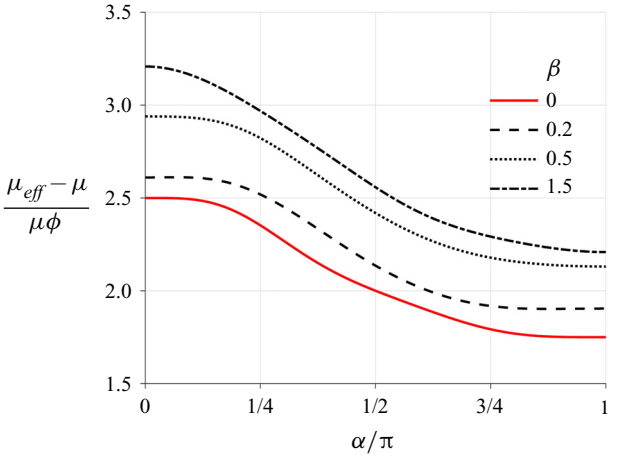

Figure 10. Plot of the $O(\phi)$ viscosity correction calculated from (6.16) against the stick–slip division angle α for a dipolar suspension of two-faced stick–slip spheres: $\lambda^+ - \lambda^- = 0.2$; $\lambda^- = 0$; $\chi = \pi/4$. Note here that when $\beta \neq 0$, every data point at a particular value of α is computed using (6.13) with the corresponding fixed orientation angles (θ_s, φ_s) obtained from the orientational dynamics like figure 8.

Adding the couple-induced bulk stress (6.12) to the couple-free bulk stress (5.10) to give the total bulk stress for the present dipolar stick–slip suspension. As a result, the effective viscosity is the Einstein viscosity (5.11),

$$\mu_{eff}^{E} = 1 + \phi\left[\frac{5}{2}\left(\frac{1+2\hat{\lambda}}{1+5\hat{\lambda}}\right) + \frac{1}{2}\left(c_1 + \frac{1}{2}\,c_2 \sin^4\theta \sin^2 2\varphi + c_3 \sin^2\theta\right)\right], \tag{6.15}$$

plus the dipolar viscosity (6.13), giving

$$\begin{aligned}\frac{\mu_{eff}}{\mu} &= (\mu_{eff}^{(E)} + \mu_{eff}^{(d)})/\mu \\ &= 1 + \phi\left[\frac{5}{2}\left(\frac{1+2\hat{\lambda}}{1+5\hat{\lambda}}\right) + 3\beta \sin\theta \sin\varphi \sin\chi\right] + \frac{1}{2}\phi\left[c_1 + \frac{1}{2}\,c_2 \sin^4\theta \sin^2 2\varphi + c_3 \sin^2\theta\right. \\ &\quad \left. + 2\beta c_4(1+3\hat{\lambda}) \sin\theta\left(\sin\varphi(2\sin^2\theta\cos^2\varphi - 1)\sin\chi + \frac{1}{2}\sin 2\theta \sin 2\varphi \cos\chi\right)\right].\end{aligned} \tag{6.16}$$

For a dipolar suspension made of two-faced stick–slip spheres with c_n given by (5.6), figure 10 shows that the $O(\phi)$ viscosity correction calculated from (6.16) basically decreases as the slip portion is increased with the stick–slip division angle α. Note here that when $\beta \neq 0$ every value of α has its own fixed orientation angles (θ_s, φ_s) obtained from the orientational dynamics like in figure 8. In addition, compared with (5.11) for the couple-free case ($\beta = 0$), the viscosity of the dipolar case ($\beta \neq 0$) is always higher, regardless of the stick–slip partition because of the additional dissipation caused by the applied external couple.

The first and second normal stress differences of the dipolar stick–slip suspension can be obtained by combining the straining part (5.10*b–d*) and the dipolar part (6.14):

$$N_1 = \mu\dot{\gamma}\phi\ \tfrac{1}{4}c_2 \sin^4\theta \sin 4\varphi + N_1^{(d)}, \tag{6.17a}$$

$$N_2 = \mu\dot{\gamma}\phi\ \tfrac{1}{2}[c_2(\sin^2\theta \sin^2\varphi - \cos^2\theta) + c_3] + N_2^{(d)}. \tag{6.17b}$$

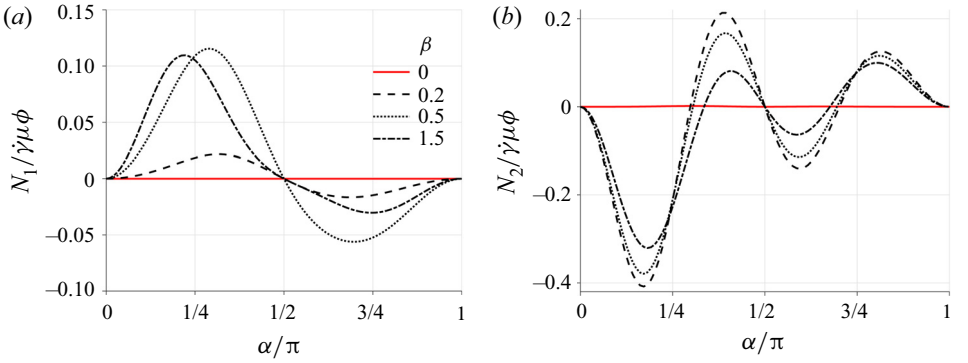

Figure 11. Typical plots of how both N_1 and N_2 vary with the stick–slip division angle α for a dipolar suspension of two-faced stick–slip spheres: $\lambda^+ - \lambda^- = 0.2$; $\lambda^- = 0$; $\chi = \pi/4$. When $\beta \neq 0$, these normal stress differences at a particular value of α are evaluated using (6.17) with the corresponding fixed orientational angles (θ_s, φ_s) obtained from the orientational dynamics like figure 8.

Compared with at most $O(\phi\varepsilon^2)$ shown by (5.12) for the couple-free case, the normal stress differences (6.17) are $O(\phi\varepsilon)$ because all the dipolar stick–slip spheres in the suspension orient in the same direction. While N_1 and N_2 are constituted by both quadrupole and hexadecapole contributions, they are made of different contributions in the anisotropic part of the stresslet (5.4), namely N_1 consists of c_2 and c_4 whereas N_2 can further involve c_3. Recall that $N_1^{(d)}$ and $N_2^{(d)}$ are made only of c_4. For this reason, by analysing how N_1 and N_2 vary with these anisotropic stresslet contributions and how these normal stress differences change with β that controls the strength of the dipolar contributions and the spheres' orientations, one may be able to extract the strengths of the quadrupole and hexadecapole to quantify their contributions to the stick–slip patterns of the spheres.

Figure 11 displays typical plots of how both N_1 and N_2 vary with the stick–slip division angle α for a dipolar suspension of two-faced stick–slip spheres. Again, for a given non-zero value of β, these normal stress differences at a particular value of α are evaluated using (6.17) with the corresponding fixed orientational angles (θ_s, φ_s) obtained from the orientational dynamics like in figure 8. Figure 11(*a*) shows that $N_1 > 0 (< 0)$ when the spheres are covered more with the stick (slip) faces with $\alpha < \pi/2 (> \pi/2)$. Note that $N_1 = 0$ at $\beta = 0$ because of (5.12*a*). A similar behaviour can also be seen for N_2, as shown in figure 11(*b*). Note that at $\beta = 0$, $\langle N_2 \rangle$ is actually very small according to figure 7(*b*).

7. Conclusions and perspectives

In this work, we have devised a new theoretical framework enabling us to systematically quantify the anisotropic nature of the stresslet of a weakly stick–slip sphere. Making use of the Lorentz reciprocal theorem joint with surface harmonic expansion, this framework allows us to come up with an extended Faxén stresslet formula, capable of describing the stresslet for the sphere with an arbitrary axisymmetric stick–slip pattern in an arbitrary imposed flow field. Using this framework we are able to identify how the stresslet is determined by distinct surface moments that can be used to reflect a variety of stick–slip symmetries/asymmetries. We show that the anisotropic contribution to the stresslet is made only of even surface moments: quadrupole and hexadecapole, like symmetric surface patterns of a striped type. This means that if the sphere is precisely half-faced with an antisymmetric dipole only and immersed in a simple shear flow, there will be no correction

to the stresslet at first order of small slip anisotropy, making the stresslet in this case behave like the uniform-slip one. In other words, to generate such a stresslet due to a surface dipole, it can only be done in a nonlinear flow field. The average bulk stress and effective viscosity of a suspension of couple-free stick–slip spheres are also determined by taking into account random Brownian rotation, showing quite different characteristics compared with those a suspension of near spheres (Hinch & Leal 1972).

Because the stresslet here is anisotropic, another important feature that follows is stresslet–rotation coupling. Unlike the force–rotation coupling due to a surface dipole (Premlata & Wei 2021), the stresslet–rotation coupling arises from a surface quadrupole. This coupling will make the stresslet no longer determined solely by the imposed strain field but further depend on a couple exerted on the sphere. This additional dependence of a stresslet on a couple can qualitatively change the orientational dynamics of a stick–slip sphere and in turn affect the rheology of a suspension made of such heterogeneous spheres. This is attributed to the fact that a stick–slip sphere is generally made of different materials, its natural chemical polarity may make it susceptible to possessing a permanent dipole moment to give rise to a couple upon an application of an external force field. As a result, the sphere will not only undergo a dipolar spinning, but also such spinning will cause additional stresses from both stresslet and couplet in a suspension of dipolar stick–slip spheres. We show that the orientation of a dipolar stick–slip sphere in a simple shear flow generally does not display a closed orbit that signifies a periodic tumbling or precession. Rather, it is tending in time to a fixed orientation due to a balance between the dipolar spinning and the flow vorticity. Since all the spheres in such a dipolar suspension orient in the same direction, this will make the bulk properties of the suspension qualitatively different from those of the couple-free situation under which the spheres' orientations are more susceptible to randomization by Brownian rotation. This is in particular manifested by the $O(\phi\varepsilon)$ normal stress differences for the former whereas those for the latter are $O(\phi\varepsilon^2)$ at most. Utilizing such normal stress differences with and without a couple, one may be able to extract the strengths of relevant surface moments and hence to quantify their contributions in the surface patterns of stick–slip spheres.

The present work mainly demonstrates the use of the simplified version (4.8) and (4.12) of the extended Faxén stresslet and torque relations in a simple shear flow. In this linear flow field, there are no finite-size corrections to the stresslet, allowing us to study the first impacts of $O(\phi)$ on the rheology of a dilute suspension of stick–slip spheres in terms of their volume fraction ϕ. And yet, if one wishes to examine the $O(\phi^2)$ effects due to hydrodynamic interactions between the spheres, the full expressions (4.6) and (4.11) of these relations will be needed (in conjunction with the method of reflections) to capture the correction to the stresslet of a stick–slip sphere due to the presence of its distant neighbours. In this case, the strain field experienced by one sphere, aside from the bulk strain field, will further include the disturbance strain field decaying as R^{-3} generated from another, where R is the interparticle distance between the spheres. The slip anisotropy contribution to the stresslet generated by such disturbance strain field thus varies like εR^{-3}, which can be more important than the standard Faxén stresslet correction $\sim R^{-5}$. In addition, because of the stresslet–rotation coupling, similar impacts from the disturbance vorticity field also have to be taken into consideration. Therefore, to analyse full impacts of hydrodynamic interactions on the stresslet of a stick–slip sphere due to its surrounding partners, the task will not be a straightforward extension of the studies by Batchelor & Green (1972*a*,*b*) for a suspension of no-slip spheres. Nevertheless, in a broader perspective, perhaps the value of these extended Faxén stresslet and torque relations would stand out when they join with the one for the force derived by Premlata

& Wei (2021) to provide a complete set of the Faxén formulae for tackling a variety of problems involving hydrodynamically interacting stick–slip spheres.

Last but not least, it would be appealing if the predictions of the present study can be compared with experiments. To our best knowledge, we have not found any such experiments that can be used to compare with our findings. Nonetheless, we can still suggest experiments to test our theory. Perhaps the best way to do so is to carry out rheological experiments for suspensions of stick–slip Janus particles. These particles can be made typically in an amphiphilic fashion by having hydrophilic (stick) colloids (e.g. inorganic particles) partially coated with another hydrophobic (slip) substance (e.g. polymer) (Jiang *et al.* 2008; Chen *et al.* 2019). The rheology properties of a suspension of such particles can then be measured to make a comparison with those of a suspension of no-slip or uniform-slip particles. Since such particles typically take the form of two faces in equal or unequal partition, the predicted effective viscosity and average normal stress differences shown in figures 6, 7, 10 and 11 can be used to compare with those measured from experiments. Alternatively, by fitting the data with these theoretical predictions, one can extract the average slip length and the stick–slip partition of Janus particles.

Funding. This work was supported by the Ministry of Science and Technology of Taiwan under the grant MOST 110-2811-E-006-507.

Declaration of interests. The authors report no conflict of interest.

Author ORCIDs.
A.R. Premlata https://orcid.org/0000-0001-6196-6667;
Hsien-Hung Wei https://orcid.org/0000-0002-8608-0296.

Appendix A. Expressing surface moments in terms of Legendre polynomials

The purpose of this appendix is to establish connections between the strengths of the surface moments in (3.11) and the coefficients in the Legendre expansion (3.12) for a given axisymmetric slip distribution. To do so, we start with (3.11):

$$\varepsilon f(\boldsymbol{x}) = -3\mathcal{D}\, d_i S_{1i} + (5/2)\mathcal{Q}\, d_i d_j S_{2ij} - (7/6)O\, d_i d_j d_k S_{3ijk} + (3/8)\mathcal{H}\, d_i d_j d_k d_l S_{4ijkl} + \cdots . \tag{A1}$$

Substitution of the surface harmonics S_{1i}, S_{2ij}, S_{3ijk}, and S_{4ijkl} defined in (3.6) into (A1) gives

$$\begin{aligned}\varepsilon f(\boldsymbol{x}) = {}& 3\mathcal{D}\, d_i n_i + (5/2)\mathcal{Q}\,(3 d_i n_i\, d_j n_j - d_i d_i) + (7/2)O\,(5\, d_i n_i\, d_j n_j\, d_k n_k - 3\, d_i n_i\, d_j d_j) \\ & + (9/8)\mathcal{H}\,(35\, d_i n_i\, d_j n_j\, d_k n_k\, d_l n_l + 3\, d_i d_i\, d_j d_j - 30\, d_i n_i\, d_j n_j\, d_k d_k) + \cdots . \end{aligned} \tag{A2}$$

Recognizing $d_i n_i = \cos\theta = \eta$ and $d_i d_i = 1$, (A2) can be reduced to

$$\begin{aligned}\varepsilon f(\boldsymbol{x}) &= 3\mathcal{D}\,\eta + (5/2)\mathcal{Q}\,(3\eta^2 - 1) + (7/2)O\,(5\eta^3 - 3\eta) + (9/8)\mathcal{H}\,(35\eta^4 - 30\eta^2 + 3) + \cdots . \\ &= 3\mathcal{D}\,\mathcal{P}_1(\eta) + 5\mathcal{Q}\,\mathcal{P}_2(\eta) + 7O\,\mathcal{P}_3(\eta) + 9\mathcal{H}\,\mathcal{P}_4(\eta) + \cdots . \end{aligned} \tag{A3}$$

Comparing (A3) with (3.12), (3.13) can be readily obtained.

Appendix B. Derivation of the Faxén stresslet relation

To make the derivations of the stresslet and torque more concise, we write the resistance tensors given by (4.1) in the more general forms for a homogeneous sphere,

$$\Sigma_{mij} = \mathbb{A}\delta_{im}n_j + \mathbb{B}n_m n_i n_j, \tag{B1a}$$

$$\Sigma^{\parallel}_{mij} = \mathbb{A}(\delta_{im}n_j - n_m n_i n_j), \tag{B1b}$$

$$R_{ij} = \mathbb{C}a^{-1}\delta_{ij}, \tag{B1c}$$

$$R^{\parallel}_{ij} = \mathbb{C}a^{-1}(\delta_{ij} - n_i n_j), \tag{B1d}$$

with the coefficients $\mathbb{A} = 5/(1+5\hat{\lambda})$, $\mathbb{B} = 40\hat{\lambda}/(1+5\hat{\lambda})$ and $\mathbb{C} = 3/(1+3\hat{\lambda})$. Hereafter we use the above wherever these tensors appear in the course of evaluating the stresslet and torque.

As given by (2.25*a*) and (2.25*b*), the stresslet comprises the uniform-slip contribution $\mathcal{S}^{(0)}_{ij}$ and the slip anisotropy correction $\mathcal{S}^{(1)}_{ij}$:

$$\mathcal{S}_{ij} = \mathcal{S}^{(0)}_{ij} + \mathcal{S}^{(1)}_{ij}, \tag{B2a}$$

$$\mathcal{S}^{(0)}_{ij} = \mu\int_{S_p}\Sigma_{mij}u^{\infty}_m \,\mathrm{d}S - a\hat{\lambda}\int_{S_p}\Sigma^{\parallel}_{mij}\sigma^{\infty}_{ml}n_l \,\mathrm{d}S, \tag{B2b}$$

$$\begin{aligned}\mathcal{S}^{(1)}_{ij} = -\varepsilon a\Bigg[&\int_{S_p} f(\boldsymbol{x})\Sigma^{\parallel}_{mij}(-p^{\infty}(0)\, n_m + \Delta^{\infty}_{ml}|_0 n_l)\,\mathrm{d}S \\ &+ \mu\int_{S_p} f(\boldsymbol{x})\Sigma^{\parallel}_{mij}\Sigma_{mpq}E^{\infty}_{pq}(0)\,\mathrm{d}S + \mu\int_{S_p} f(\boldsymbol{x})\Sigma^{\parallel}_{mij}R_{mn}\epsilon_{rsn}x_s(\Omega^{\infty}_r(0) - \Omega_r)\,\mathrm{d}S\Bigg].\end{aligned} \tag{B2c}$$

B.1. *Uniform-slip stresslet* $\mathcal{S}^{(0)}_{ij}$

Here $\mathcal{S}^{(0)}_{ij}$ given by (B2*b*) is made of two terms: the $\boldsymbol{u}^{\infty}$ term and the $\boldsymbol{\sigma}^{\infty}$ term. The former can be evaluated by expanding $\boldsymbol{u}^{\infty}$ as (4.2*a*) and by using (4.3*a–c*), giving

$$\begin{aligned}&\mu\int_{S_p} u^{\infty}_m\ \Sigma_{mij}\,\mathrm{d}S \\ &\quad= \mu\int_{S_p}(\mathbb{A}\delta_{im}n_j + \mathbb{B}n_m n_i n_j)\left[x_k\nabla_k u^{\infty}_m|_0 + \frac{x_p x_q x_r}{3!}\nabla_p\nabla_q\nabla_r u^{\infty}_m|_0 + \cdots\right]\mathrm{d}S \\ &\quad= \pi\mu a^3\left[\frac{4}{3}\mathbb{A}\delta_{jk}\delta_{im} + \frac{4}{15}\mathbb{B}A_{ijkm}\right]\nabla_k u^{\infty}_m(0) \\ &\qquad+ \frac{1}{6}\pi\mu a^5\left[\frac{4}{15}\mathbb{A}\,A_{jpqr}\delta_{im} + \frac{4}{105}\mathbb{B}\,B_{ijmpqr}\right]\nabla_p\nabla_q\nabla_r u^{\infty}_m|_0 \\ &\qquad= \frac{4}{3}\pi\mu a^3\left[\mathbb{A} + \frac{2\mathbb{B}}{5}\right]E^{\infty}_{ij}|_0 + \frac{2}{15}\pi\mu a^5\left[\mathbb{A} + \frac{2\mathbb{B}}{7}\right]\nabla^2 E^{\infty}_{ij}|_0.\end{aligned} \tag{B3}$$

In the above, we have used $\nabla_i u^{\infty}_i = 0$ and $E^{\infty}_{ij} = (1/2)(\nabla_i u^{\infty}_j + \nabla_j u^{\infty}_i)$.

For the $\boldsymbol{\sigma}^{\infty}$ term, we can evaluate by expanding σ^{∞}_{jk} as (4.2*b*) followed by the use of (4.3*a*)–(4.3*c*), yielding

$$
\begin{aligned}
&-a\hat{\lambda}\int_{S_p}\Sigma^{\parallel}_{mij}\sigma^{\infty}_{ml}n_l\,\mathrm{d}S\\
&\quad=-a\hat{\lambda}\int_{S_p}\mathbb{A}(\delta_{im}n_j-n_mn_in_j)\left[\sigma^{\infty}_{mk}(0)+\frac{x_px_q}{2!}\nabla_p\nabla_q\sigma^{\infty}_{mk}\big|_0+\cdots\right]n_k\,\mathrm{d}S\\
&\quad=-\pi a^3\hat{\lambda}\mathbb{A}\left[\frac{4}{3}\delta_{im}\delta_{jk}-\frac{4}{15}A_{ijmk}\right]\sigma^{\infty}_{mk}(0)\\
&\qquad-\frac{1}{2}\pi a^5\hat{\lambda}\mathbb{A}\left[\frac{4}{15}A_{jkpq}\delta_{im}-\frac{4}{105}B_{ijmkpq}\right]\nabla_p\nabla_q\sigma^{\infty}_{mk}\big|_0\\
&\quad=-\frac{4}{5}\pi\mu a^3\hat{\lambda}\mathbb{A}\left(\sigma^{\infty}_{ij}(0)-\frac{1}{3}\delta_{ij}\sigma^{\infty}_{mm}(0)\right)-\frac{2}{21}\pi\mu a^5\hat{\lambda}\mathbb{A}\left(\nabla^2\sigma^{\infty}_{ij}\big|_0-\frac{2}{5}\nabla_i\nabla_j\sigma^{\infty}_{mm}\big|_0\right).
\end{aligned}
\tag{B4}
$$

In deriving (B4), we have used $\nabla_i\sigma^{\infty}_{ij}=0$. Combining (B3) and (B4) by recognizing that $\sigma^{\infty}_{ij}=-p^{\infty}\delta_{ij}+2\mu E^{\infty}_{ij}$, $\sigma^{\infty}_{mm}=-3p^{\infty}$ and $\nabla_i\nabla_j\sigma^{\infty}_{mm}=-3\nabla_i\nabla_jp^{\infty}=-3\mu\nabla^2E^{\infty}_{ij}$, (B2*b*) becomes

$$
\mathcal{S}^{(0)}_{ij}=\frac{4}{3}\pi\mu a^3\left[\mathbb{A}+\frac{2}{5}(\mathbb{B}-3\hat{\lambda}\mathbb{A})\right]E^{\infty}_{ij}\big|_0+\frac{2}{15}\pi\mu a^5\mathbb{A}\nabla^2E^{\infty}_{ij}\big|_0,
\tag{B5}
$$

which is (4.4).

B.2. *Anisotropic stresslet* $\mathcal{S}^{(1)}_{ij}$

The slip anisotropy correction (B2*c*) is made of surface dipole, quadrupole, octupole and hexadecapole contributions: $\mathcal{S}^{(1)}_{ij}=\mathcal{S}^{D}_{ij}+\mathcal{S}^{Q}_{ij}+\mathcal{S}^{O}_{ij}+\mathcal{S}^{H}_{ij}$. Each contribution is evaluated separately as follows.

B.2.1. *Dipole stresslet* $\mathcal{S}^{D}_{ij}$

$$
\mathcal{S}^{D}_{ij}=-a\int_{S_p}\varepsilon f(\boldsymbol{x})\;\Sigma^{\parallel}_{mij}(-p^{\infty}(0)\,n_m+\Delta^{\infty}_{ml}\big|_0\,n_l)\,\mathrm{d}S,
\tag{B6}
$$

with

$$
\varepsilon f(\boldsymbol{x})=3\langle\lambda S_{1k}\rangle S_{1k}=3P_{1k}n_k.
\tag{B7}
$$

The contribution from $p^{\infty}(0)$ is identically zero. For the contribution from Δ^{∞} that represents the stress gradient terms in the expansion (4.2*b*), it can be evaluated using

(4.3*b*,*c*), which turns (B6) into

$$\begin{aligned}\mathcal{S}_{ij}^{D} &= -a\mathbb{A}\int_{S_p} 3P_{1k}n_k(\delta_{im}n_j - n_m n_i n_j)\left(x_n\nabla_n\sigma_{ml}^{\infty}\big|_0 n_l + \cdots\right)\mathrm{d}S \\ &= -3\pi a^4\mathbb{A}\,P_{1k}\left[\frac{4}{15}A_{jkln}\delta_{im} - \frac{4}{105}B_{ijklmn}\right]\nabla_n\sigma_{ml}^{\infty}\big|_0 \\ &= -\frac{4}{7}\pi a^4\mathbb{A}\,P_{1k}\left[\nabla_k\sigma_{ij}^{\infty}\big|_0 + \frac{3}{10}\left(\nabla_i\sigma_{jk}^{\infty}\big|_0 + \nabla_j\sigma_{ik}^{\infty}\big|_0\right)\right. \\ &\quad \left. - \frac{1}{5}\left(\delta_{ik}\nabla_j\sigma_{mm}^{\infty}\big|_0 + \delta_{jk}\nabla_i\sigma_{mm}^{\infty}\big|_0 + \delta_{ij}\nabla_k\sigma_{mm}^{\infty}\big|_0\right)\right]. \end{aligned} \tag{B8}$$

In deriving the above, we have used $\nabla_i\sigma_{ij}^{\infty} = 0$. Further making use of the relations $\sigma_{ij}^{\infty} = -p^{\infty}\delta_{ij} + 2\mu E_{ij}^{\infty}$, $\sigma_{mm}^{\infty} = -3p^{\infty}$ and $\nabla_i p^{\infty} = 2\mu\nabla_k E_{ik}^{\infty}$, (B8) is reduced to (4.5*a*).

B.2.2. *Quadrupole stresslet* $\mathcal{S}_{ij}^{Q}$

The quadrupole stresslet $\mathcal{S}_{ij}^{Q}$ consists of three contributions according to

$$\mathcal{S}_{ij}^{Q} = \mathcal{S}_{ij}^{Q1} + \mathcal{S}_{ij}^{Q2} + \mathcal{S}_{ij}^{Q3}, \tag{B9a}$$

$$\mathcal{S}_{ij}^{Q1} = -a\mu\int_{S_p}\varepsilon f(\boldsymbol{x})\,\Sigma_{mij}^{\parallel}\Sigma_{mlk}E_{lk}^{\infty}(0)\,\mathrm{d}S, \tag{B9b}$$

$$\mathcal{S}_{ij}^{Q2} = -a\mu\int_{S_p}\varepsilon f(\boldsymbol{x})\,\Sigma_{mij}^{\parallel}R_{mn}\epsilon_{rsn}x_s(\Omega_r^{\infty}(0) - \Omega_r)\,\mathrm{d}S, \tag{B9c}$$

$$\mathcal{S}_{ij}^{Q3} = -a\int_{S_p}\varepsilon f(\boldsymbol{x})\,\Sigma_{mij}^{\parallel}(-p^{\infty}(0)n_m + \Delta_{ml}^{\infty}\big|_0 n_l)\,\mathrm{d}S, \tag{B9d}$$

wherein

$$\varepsilon f(\boldsymbol{x}) = (5/6)\langle\lambda S_{2pq}\rangle S_{2pq} = (5/6)P_{2pq}(3n_p n_q - \delta_{pq}). \tag{B10}$$

Equation (B9*b*) can be calculated as

$$\begin{aligned}\mathcal{S}_{ij}^{Q1} &= -a\mu(5/6)\langle\lambda S_{2pq}\rangle\int_{S_p} S_{2pq}\,\Sigma_{mij}^{\parallel}\Sigma_{mlk}\,E_{lk}^{\infty}(0)\,\mathrm{d}S \\ &= -a\mu(5/6)P_{2pq}\int_{S_p}\mathbb{A}^2(\delta_{il}n_j n_k - n_i n_j n_k n_l)(3n_p n_q - \delta_{pq})E_{lk}^{\infty}(0)\,\mathrm{d}S \\ &= -\frac{5}{2}\pi\mu a^3\mathbb{A}^2\,P_{2pq}\left[\frac{4}{15}\delta_{il}A_{jkpq} - \frac{4}{105}B_{ijklpq}\right]E_{lk}^{\infty}(0) \\ &= -\frac{2}{7}\pi\mu a^3\mathbb{A}^2\,P_{2lk}\left[\delta_{ik}E_{jk}^{\infty}(0) + \delta_{jk}E_{ik}^{\infty}(0) - \frac{2}{3}\delta_{ij}E_{lk}^{\infty}(0)\right]. \end{aligned} \tag{B11}$$

In arriving at the above, we have used $\delta_{pq}P_{2pq}=0$. Similarly, (B9*c*) can be evaluated as

$$\begin{aligned}\mathcal{S}_{ij}^{Q2} &= -a\mu(5/6)\langle\lambda S_{2pq}\rangle\int_{S_p} S_{2pq}\Sigma^{\parallel}_{mij}R_{mn}\,\epsilon_{rsn}x_s(\Omega_r^{\infty}(0)-\Omega_r)\,\mathrm{d}S\\ &= -\mu(5/6)P_{2pq}\int_{S_p}\mathbb{AC}(\delta_{in}n_j-n_nn_in_j)(3n_pn_q-\delta_{pq})\epsilon_{nrs}x_s(\Omega_r^{\infty}(0)-\Omega_r)\,\mathrm{d}S\\ &= -\frac{5}{2}\pi\mu a^3\mathbb{AC}\;P_{2pq}\left[\frac{4}{15}\delta_{in}A_{jpqs}-\frac{4}{105}B_{nijpqs}\right]\epsilon_{nrs}(\Omega_r^{\infty}(0)-\Omega_r)\\ &= -\frac{2}{3}\pi\mu a^3\mathbb{AC}\left[\epsilon_{irp}P_{2jp}+\epsilon_{jrp}P_{2ip}\right](\Omega_r^{\infty}(0)-\Omega_r).\end{aligned}\tag{B12}$$

Equation (B9*d*) can be computed in a manner similar to (B6), yielding

$$\begin{aligned}\mathcal{S}_{ij}^{Q3} &= -a(5/6)\langle\lambda S_{2pq}\rangle\int_{S_p} S_{2pq}\Sigma^{\parallel}_{mij}\left(-p^{\infty}(0)n_m+\frac{x_nx_k}{2!}\nabla_n\nabla_k\sigma^{\infty}_{ml}\big|_0\,n_l+\cdots\right)\mathrm{d}S\\ &= -\frac{5}{6}aP_{2pq}\int_{S_p}\mathbb{A}(\delta_{im}n_j-n_mn_in_j)(3n_pn_q-\delta_{pq})(\frac{x_nx_k}{2!}\nabla_n\nabla_k\sigma^{\infty}_{ml}\big|_0n_l+\cdots)\,\mathrm{d}S\\ &= -\frac{5}{2}\pi a^5\mathbb{A}P_{2pq}\left[\frac{4}{105}\delta_{im}B_{jklnpq}-\frac{4}{945}C_{ijklmnpq}\right]\nabla_n\nabla_k\sigma^{\infty}_{ml}\big|_0\\ &= -\frac{2}{189}\pi a^5\mathbb{A}P_{2pq}\left[\frac{5}{2}\left(\delta_{ip}\nabla^2\sigma^{\infty}_{jq}\big|_0+\delta_{jp}\nabla^2\sigma^{\infty}_{iq}\big|_0\right)-\delta_{ij}\nabla^2\sigma^{\infty}_{pq}\big|_0\right.\\ &\quad+5(\nabla_p\nabla_j\sigma^{\infty}_{iq}\big|_0+\nabla_p\nabla_i\sigma^{\infty}_{jq}\big|_0)+7\nabla_p\nabla_q\sigma^{\infty}_{ij}\big|_0-2\nabla_i\nabla_j\sigma^{\infty}_{pq}\big|_0\\ &\quad\left.-2(\delta_{ip}\nabla_q\nabla_j\sigma^{\infty}_{mm}\big|_0+\delta_{jp}\nabla_q\nabla_i\sigma^{\infty}_{mm}\big|_0+\frac{1}{2}\delta_{ij}\nabla_p\nabla_q\sigma^{\infty}_{mm}\big|_0)\right].\end{aligned}\tag{B13}$$

Writing σ^{∞}_{ij} and σ^{∞}_{mm} in terms of E^{∞}_{ij} using the relations below (B8), (B13) can be simplified to

$$\begin{aligned}\mathcal{S}_{ij}^{Q3} &= -\frac{4}{189}\pi\mu a^5\mathbb{A}\;P_{2pq}[3(\delta_{ip}\nabla^2E^{\infty}_{jq}\big|_0+\delta_{jp}\nabla^2E^{\infty}_{iq}\big|_0-\delta_{ij}\nabla^2E^{\infty}_{pq}\big|_0)\\ &\quad+5(\nabla_p\nabla_jE^{\infty}_{iq}\big|_0+\nabla_p\nabla_iE^{\infty}_{jq}\big|_0)+7\nabla_p\nabla_qE^{\infty}_{ij}\big|_0-2\nabla_i\nabla_jE^{\infty}_{pq}\big|_0].\end{aligned}\tag{B14}$$

Combining (B11), (B12) and (B14) gives (4.5*b*).

B.2.3. *Octupole stresslet* $\mathcal{S}^{O}_{ij}$

$$\mathcal{S}^{O}_{ij}=-a\int_{S_p}\varepsilon f(\boldsymbol{x})\Sigma^{\parallel}_{mij}(-p^{\infty}(0)\,n_m+\Delta^{\infty}_{ml}\big|_0\,n_l)\,\mathrm{d}S,\tag{B15}$$

with

$$\begin{aligned}\varepsilon f(\boldsymbol{x}) &= (7/90)\langle\lambda S_{3kpq}\rangle S_{3kpq}\\ &= (7/90)P_{3kpq}(15n_kn_pn_q-3(n_k\delta_{pq}+n_p\delta_{kq}+n_q\delta_{kp})).\end{aligned}\tag{B16}$$

In (B16), $3(n_k\delta_{pq}+n_p\delta_{kq}+n_q\delta_{kp})P_{3kpq}=0$. Like $\mathcal{S}_{ij}^{Q3}$ shown by (B13), $\mathcal{S}_{ij}^{O}$ can be evaluated as

$$\begin{aligned}\mathcal{S}_{ij}^{O} &= -a(7/90)\langle\lambda S_{3kpq}\rangle\int_{S_p} S_{3kpq}\Sigma^{\parallel}_{mij}(-p^{\infty}(0)n_m + x_n\nabla_n\sigma^{\infty}_{ml}\big|_0\, n_l+\cdots)\,\mathrm{d}S\\ &= -(7/90)aP_{3kpq}\int_{S_p} 15n_kn_pn_q\Sigma^{\parallel}_{mij}(x_n\nabla_n\sigma^{\infty}_{ml}\big|_0\, n_l+\cdots)\,\mathrm{d}S\\ &= -\frac{7}{6}a\mathbb{A}P_{3kpq}\int_{S_p} n_kn_pn_q(\delta_{im}n_j-n_mn_in_j)x_n\nabla_n\sigma^{\infty}_{ml}\big|_0\, n_l\\ &= -\frac{7}{6}\pi a^4\mathbb{A}P_{3kpq}\left[\frac{4}{105}\delta_{im}B_{jklnpq}-\frac{4}{945}C_{ijklnpq}\right]\nabla_n\sigma^{\infty}_{ml}\big|_0\\ &= -\frac{4}{135}\pi a^4\mathbb{A}\Big[\frac{5}{2}\left(P_{3imn}\nabla_n\sigma^{\infty}_{jm}\big|_0+P_{3jmn}\nabla_n\sigma^{\infty}_{im}\big|_0\right)\\ &\quad-\left(\delta_{ij}P_{3mnl}\nabla_n\sigma^{\infty}_{ml}\big|_0+P_{3ijn}\nabla_n\sigma^{\infty}_{mm}\big|_0+P_{3jmn}\nabla_i\sigma^{\infty}_{mn}\big|_0+P_{3imn}\nabla_j\sigma^{\infty}_{mn}\big|_0\right)\Big].\end{aligned}\tag{B17}$$

Written in terms of E^{∞}_{ij}, (B17) can be reduced to

$$\begin{aligned}\mathcal{S}_{ij}^{O} = -\frac{8}{135}\pi\mu a^4\mathbb{A}\Big[&\frac{5}{2}\left(P_{3imn}\nabla_nE^{\infty}_{jm}\big|_0+P_{3jmn}\nabla_nE^{\infty}_{im}\big|_0\right)-\delta_{ij}P_{3mnl}\nabla_nE^{\infty}_{ml}\big|_0\\ &-P_{3imn}\nabla_jE^{\infty}_{mn}\big|_0-P_{3jmn}\nabla_iE^{\infty}_{mn}\big|_0-2P_{3ijn}\nabla_kE^{\infty}_{nk}\big|_0\Big],\end{aligned}\tag{B18}$$

which is (4.5*c*).

B.2.4. *Hexadecapole stresslet* $\mathcal{S}_{ij}^{H}$

$$\mathcal{S}_{ij}^{H} = -a\mu\int_{S_p}\varepsilon f(\boldsymbol{x})\,\Sigma^{\parallel}_{mij}\,\Sigma_{mlk}E^{\infty}_{lk}(0)\,\mathrm{d}S,\tag{B19}$$

with

$$\begin{aligned}\varepsilon f(\boldsymbol{y}) &= (1/280)\langle\lambda S_{4pqrs}\rangle S_{4pqrs}\\ &= (1/280)P_{4pqrs}[105n_pn_qn_rn_s+3A_{pqrs}\\ &\quad-15(n_pn_q\delta_{rs}+n_pn_r\delta_{qs}+n_pn_s\delta_{qr}+n_qn_r\delta_{ps}+n_qn_s\delta_{pr}+n_rn_s\delta_{pq})].\end{aligned}\tag{B20}$$

In (B20), $[3A_{pqrs}-15(n_pn_q\delta_{rs}+n_pn_r\delta_{qs}+n_pn_s\delta_{qr}+n_qn_r\delta_{ps}+n_qn_s\delta_{pr}+n_rn_s\delta_{pq})]P_{4pqrs}=0$. Equation (B19) can be evaluated as

$$\begin{aligned}\mathcal{S}_{ij}^{H} &= -a\mu(1/280)\langle\lambda S_{4pqrs}\rangle\int_{S_p} S_{4pqrs}\,\Sigma^{\parallel}_{mij}\Sigma_{mlk}E^{\infty}_{lk}(0)\,\mathrm{d}S\\ &= -a\mu(1/280)P_{4pqrs}\int_{S_p}\mathbb{A}^2(\delta_{il}n_jn_k-n_in_jn_kn_l)105n_pn_qn_rn_sE^{\infty}_{lk}(0)\,\mathrm{d}S\\ &= -\frac{3}{8}\pi\mu a^3\mathbb{A}^2P_{4pqrs}\left[\frac{4}{105}\delta_{il}B_{pqrsjk}-\frac{4}{945}C_{ijklpqrs}\right]E^{\infty}_{lk}(0)\\ &= \frac{4}{105}\pi\mu a^3\mathbb{A}^2P_{4ijlk}E^{\infty}_{lk}(0),\end{aligned}\tag{B21}$$

which is (4.5*d*).

Appendix C. Derivation of the Faxén torque relation

Similar to the stresslet, the derivation of the torque involves the uniform-slip part $\mathcal{L}_k^{(0)}$ (2.25*c*) and the slip anisotropy correction $\mathcal{L}_k^{(1)}$ (2.25*d*):

$$\mathcal{L}_k = \mathcal{L}_k^{(0)} + \mathcal{L}_k^{(1)}, \tag{C1a}$$

$$\mathcal{L}_k^{(0)} = \mu \int_{S_p} \epsilon_{kln} x_l \left[R_{mn} u_m^\infty - R_{qn} \epsilon_{qrs} \Omega_r x_s \right] \mathrm{d}S - a\hat{\lambda} \int_{S_p} \epsilon_{kln} x_l R_{mn}^{\parallel} \sigma_{mj}^\infty n_j \, \mathrm{d}S, \tag{C1b}$$

$$\mathcal{L}_k^{(1)} = -\varepsilon a \Bigg[\int_{S_p} f(\boldsymbol{x}) \epsilon_{kln} x_l \, R_{mn}^{\parallel} (-p^\infty(0) \, n_m + \Delta_{mq}^\infty\big|_0 \, n_q) \, \mathrm{d}S + \mu \int_{S_p} f(\boldsymbol{x}) \, \epsilon_{kln} x_l \, R_{mn}^{\parallel} \Sigma_{mpq} E_{pq}^\infty(0) \, \mathrm{d}S + \mu \int_{S_p} f(\boldsymbol{x}) \, \epsilon_{kln} \epsilon_{rsq} x_l x_s \, R_{mn}^{\parallel} R_{mq} (\Omega_r^\infty(0) - \Omega_r) \, \mathrm{d}S \Bigg]. \tag{C1c}$$

These two contributions are evaluated separately below.

C.1. *Uniform-slip part* $\mathcal{L}_k^{(0)}$

Here $\mathcal{L}_k^{(0)}$ given by (C1*a*) is made of the body rotation term ($\boldsymbol{u}^\infty - \boldsymbol{\Omega} \times \boldsymbol{x}$) and the $\boldsymbol{\sigma}^\infty$ term. For the former, it can be evaluated below by expanding $\boldsymbol{u}^\infty$ as (4.2*a*) and using (4.3*a*,*b*):

$$\begin{aligned} &\mu \int_{S_p} \epsilon_{kln} x_l \left[R_{mn} u_m^\infty - R_{qn} \epsilon_{qrs} \Omega_r x_s \right] \mathrm{d}S \\ &= \frac{\mathbb{C}}{a} \mu \int_{S_p} \epsilon_{kln} \, x_l \, \left[\delta_{mn} \left(x_p \nabla_p u_m^\infty\big|_0 + \cdots \right) - \delta_{qn} \epsilon_{qrs} \Omega_r x_s \right] \mathrm{d}S \\ &= \frac{4}{3} \mathbb{C} \pi \mu a^3 \left[\epsilon_{kpm} \nabla_p u_m^\infty\big|_0 - 2\Omega_k \right] \\ &= \frac{8}{3} \mathbb{C} \pi \mu a^3 \left(\Omega_k^\infty(0) - \Omega_k \right). \end{aligned} \tag{C2}$$

The $\boldsymbol{\sigma}^\infty$ term is evaluated by expanding $\boldsymbol{\sigma}^\infty$ as (4.2*b*) followed by the use of (4.3*a*)–(4.3*c*). We find that this term is identically zero (Premlata & Wei 2021).

C.2. *Slip anisotropy correction* $\mathcal{L}_k^{(1)}$

The slip anisotropy correction given by (C1*c*) is constituted by surface dipole, quadrupole, and octupole contributions: $\mathcal{L}_k^{(1)} = \mathcal{L}_k^D + \mathcal{L}_k^Q + \mathcal{L}_k^O$. Below are separate evaluations for these different contributions.

C.2.1. *Dipole torque* $\mathcal{L}_k^D$

$$\mathcal{L}_k^D = -a\int_{S_p} \varepsilon f(\boldsymbol{x})\epsilon_{kln}x_l R^{\parallel}_{mn}(-p^{\infty}(0)\ n_m + \Delta^{\infty}_{ml}\big|_0 n_l)\,\mathrm{d}S, \tag{C3}$$

with $\varepsilon f(\boldsymbol{x})$ given by (B7). Similar to the procedures to compute the dipole stresslet $\mathcal{S}_{ij}^D$ (B6), (C3) can be evaluated as

$$\begin{aligned}
\mathcal{L}_k^D &= -\varepsilon a\int_{S_p} f(\boldsymbol{x})\epsilon_{kln}x_l\ R^{\parallel}_{mn}\ (-p^{\infty}(0)\ n_m + \Delta^{\infty}_{mq}\big|_0\ n_q)\,\mathrm{d}S \\
&= -3a\mathbb{C}\langle\lambda S_{1j}\rangle\int_{S_p}\epsilon_{kln}\ n_l n_j(\delta_{mn}-n_m n_n)(x_p\nabla_p\sigma^{\infty}_{mq}\big|_0\ n_q+\cdots)\,\mathrm{d}S \\
&= -3\pi a^4\mathbb{C}\ P_{1j}\epsilon_{kln}\left[\frac{4}{15}\delta_{mn}A_{jlpq}-\frac{4}{105}B_{mnjlpq}\right]\nabla_p\sigma^{\infty}_{mq}\big|_0 \\
&= -\frac{4}{5}\pi a^4\mathbb{C}\ P_{1j}\epsilon_{kmn}\nabla_m\sigma^{\infty}_{jn}\big|_0.
\end{aligned} \tag{C4}$$

Using $\sigma^{\infty}_{ij} = -p^{\infty}\delta_{ij} + 2\mu E^{\infty}_{ij}$ and $\nabla_i p^{\infty} = 2\mu\nabla_k E^{\infty}_{ik}$, the above can be reduced to (4.10*a*).

C.2.2. *Quadrupole torque* $\mathcal{L}_k^Q$

The quadrupole torque $\mathcal{L}_k^Q$ is made of three contributions,

$$\mathcal{L}_k^Q = \mathcal{L}_k^{Q1} + \mathcal{L}_k^{Q2} + \mathcal{L}_k^{Q3}, \tag{C5a}$$

$$\mathcal{L}_k^{Q1} = -a\mu\int_{S_p}\varepsilon f(\boldsymbol{x})\ \epsilon_{kln}x_l R^{\parallel}_{mn}\Sigma_{mpq}E^{\infty}_{pq}(0)\,\mathrm{d}S, \tag{C5b}$$

$$\mathcal{L}_k^{Q2} = -a\mu\int_{S_p}\varepsilon f(\boldsymbol{x})\ \epsilon_{kln}\epsilon_{rsq}\ x_l x_s\ \ R^{\parallel}_{mn}R_{mq}(\Omega^{\infty}_r(0)-\Omega_r)\,\mathrm{d}S, \tag{C5c}$$

$$\mathcal{L}_k^{Q3} = -a\int_{S_p}\varepsilon f(\boldsymbol{x})\ \epsilon_{kln}x_l\ R^{\parallel}_{mn}\ (-p^{\infty}(0)\ n_m + \Delta^{\infty}_{mq}\big|_0\ n_q)\,\mathrm{d}S, \tag{C5d}$$

wherein $\varepsilon f(\boldsymbol{x})$ is given by (B10). Using (4.3), these different contributions can be evaluated as follows:

$$\begin{aligned}
\mathcal{L}_k^{Q1} &= -a\mu(5/6)\langle\lambda S_{2ij}\rangle\int_{S_p} S_{2ij}\ \epsilon_{kln}x_l R^{\parallel}_{mn}\Sigma_{mpq}E^{\infty}_{pq}(0)\,\mathrm{d}S \\
&= -\frac{5}{6}\mu a\mathbb{A}\mathbb{C}\ P_{2ij}\int_{S_p}\epsilon_{kln}n_l(3n_in_j-\delta_{ij})(\delta_{np}n_q-n_nn_pn_q)E^{\infty}_{pq}(0)\,\mathrm{d}S \\
&= -\frac{5}{2}\pi\mu a^3\mathbb{A}\mathbb{C}\ P_{2ij}\epsilon_{kln}\left[\frac{4}{15}\delta_{np}A_{ijql}-\frac{4}{105}B_{ijpqnl}\right]E^{\infty}_{pq}(0) \\
&= -\frac{4}{3}\pi\mu a^3\mathbb{A}\mathbb{C}\ \epsilon_{kmn}P_{2mj}E^{\infty}_{jn}(0),
\end{aligned} \tag{C6}$$

$$\begin{aligned}\mathcal{L}_k^{Q2} &= -a\mu(5/6)\langle\lambda S_{2ij}\rangle\int_{S_p} S_{2ij}\,\epsilon_{kln}\epsilon_{rsq}\,x_l x_s\;\; R^{\parallel}_{mn}R_{mq}(\Omega_r^{\infty}(0)-\Omega_r)\,\mathrm{d}S\\ &= -\frac{5}{6}\mu a\mathbb{C}^2\,P_{2ij}\int_{S_p}\epsilon_{kln}\epsilon_{rsq}\,n_l n_s(3n_in_j-\delta_{ij})(\delta_{qn}-n_qn_n)(\Omega_r^{\infty}(0)-\Omega_r)\,\mathrm{d}S\\ &= -\frac{5}{2}\pi\mu a^3\mathbb{C}^2\,P_{2ij}\,\epsilon_{kln}\epsilon_{rsq}\left[\frac{4}{15}\delta_{qn}A_{ijls}-\frac{4}{105}B_{ijqnls}\right](\Omega_r^{\infty}(0)-\Omega_r)\\ &= \frac{4}{3}\pi\mu a^3\mathbb{C}^2\,P_{2kr}(\Omega_r^{\infty}(0)-\Omega_r),\end{aligned}\tag{C7}$$

$$\begin{aligned}\mathcal{L}_k^{Q3} &= -a(5/6)\langle\lambda S_{2ij}\rangle\int_{S_p} S_{2ij}\;\;\epsilon_{kln}x_l\,R^{\parallel}_{mn}\,(-p^{\infty}(0)\,n_m+\Delta^{\infty}_{mr}|_0\,n_r)\,\mathrm{d}S\\ &= -\frac{5}{6}a\mathbb{C}\,P_{2ij}\int_{S_p}\epsilon_{kln}n_l(3n_in_j-\delta_{ij})(\delta_{mn}-n_mn_n)\;\left(\frac{x_px_q}{2!}\nabla_p\nabla_q\sigma^{\infty}_{mr}|_0\,n_r+\cdots\right)\mathrm{d}S\\ &= -\frac{5}{4}\pi a^5\mathbb{C}\,P_{2ij}\epsilon_{kln}\left[\frac{4}{105}\delta_{mn}B_{ijpqrl}-\frac{4}{945}C_{ijpqmnlr}\right]\nabla_p\nabla_q\sigma^{\infty}_{mr}|_0\\ &= -\frac{2}{21}\pi a^5\mathbb{C}\epsilon_{klm}[2P_{2jr}\nabla_j\nabla_l\sigma^{\infty}_{mr}|_0+P_{2lr}\nabla^2\sigma^{\infty}_{mr}|_0].\end{aligned}\tag{C8}$$

Equation (C8) can be rewritten as the following form by writing σ_{ij}^{∞} in terms of E_{ij}^{∞} using the relations below (B8):

$$\mathcal{L}_k^{Q3} = -\frac{4}{21}\pi\mu a^5\mathbb{C}\epsilon_{klm}[2P_{2jr}\nabla_j\nabla_l E^{\infty}_{mr}|_0-2P_{2mj}\nabla_j\nabla_p E^{\infty}_{pl}|_0+P_{2lr}\nabla^2E^{\infty}_{mr}|_0].\tag{C9}$$

Combining (C6), (C7) and (C9) gives (4.10*b*).

C.2.3. *Octupole torque* $\mathcal{L}_k^O$

$$\mathcal{L}_k^O = -a\int_{S_p}\varepsilon f(\boldsymbol{x})\epsilon_{kln}x_lR^{\parallel}_{mn}(-p^{\infty}(0)\,n_m+\Delta^{\infty}_{mr}|_0n_r)\,\mathrm{d}S,\tag{C10}$$

with $\varepsilon f(\boldsymbol{x})$ given by (B16). Similar to (C4), (C10) can be evaluated as

$$\begin{aligned}\mathcal{L}_k^O &= -a(7/90)\langle\lambda S_{3pij}\rangle\int_{S_p}S_{3pij}\epsilon_{kln}\,x_lR^{\parallel}_{mn}(-p^{\infty}(0)\,n_m+x_q\nabla_q\sigma^{\infty}_{mr}|_0\,n_r+\cdots)\,\mathrm{d}S\\ &= -(7/90)a^2P_{3ijp}\int_{S_p}15n_in_jn_p\epsilon_{kln}n_lR^{\parallel}_{mn}(x_q\nabla_q\sigma^{\infty}_{mr}|_0\,n_r+\cdots)\,\mathrm{d}S\\ &= -\frac{7}{6}a^2\mathbb{C}\,P_{3ijp}\int_{S_p}\epsilon_{kln}\,n_in_jn_pn_l(\delta_{mn}-n_mn_n)(n_q\nabla_q\sigma^{\infty}_{mr}|_0\,n_r)\\ &= -\frac{7}{6}\pi a^4\mathbb{C}\,P_{3ijp}\,\epsilon_{kln}\left[\frac{4}{105}\delta_{mn}B_{ijpqlr}-\frac{4}{945}C_{ijpqlrmn}\right]\nabla_q\sigma^{\infty}_{mr}|_0\\ &= -\frac{4}{5}\pi a^4\mathbb{C}\,P_{3jlp}\,\epsilon_{klm}\nabla_p\sigma^{\infty}_{jm}|_0.\end{aligned}\tag{C11}$$

With $\sigma_{ij}^{\infty}=-p^{\infty}\delta_{ij}+2\mu E_{ij}^{\infty}$, the above leads to (4.10*c*).

References

Anderson, J.L. 1985 Effect of nonuniform zeta potential on particle movement in electric fields. *J. Colloid Interface Sci.* **105** (1), 45–54.

Batchelor, G.K. 1970 The stress system in a suspension of force-free particles. *J. Fluid Mech.* **41** (3), 545–570.

Batchelor, G.K. & Green, J.T. 1972*a* The hydrodynamic interaction of two small freely-moving spheres in a linear flow field. *J. Fluid Mech.* **56** (2), 375–400.

Batchelor, G.K. & Green, J.T. 1972*b* The determination of the bulk stress in a suspension of spherical particles to order c^2. *J. Fluid Mech.* **56** (3), 401–427.

Blake, J.R. 1971 A spherical envelope approach to ciliary propulsion. *J. Fluid Mech.* **46** (1), 199–208.

Brenner, H. 1964 The Stokes resistance of a slightly deformed sphere. *Chem. Engng Sci.* **19** (8), 519–539.

Brenner, H. 1970 Rheology of a dilute suspension of dipolar spherical particles in an external field. *J. Colloid Interface Sci.* **32** (1), 141–158.

Bretherton, F.P. 1962 The motion of rigid particles in a shear flow at low Reynolds number. *J. Fluid Mech.* **14** (2), 284–304.

Chen, X., Xu, J., Sun, D., Jiang, B., Liang, F. & Yang, Z. 2019 Emulsion interfacial synthesis of polymer/inorganic Janus particles. *Langmuir* **35** (18), 6032–6038.

Einstein, A. 1906 A new determination of molecular dimensions. *Ann. Phys.* **19**, 289–306.

Ericksen, J.L. 1959 Anisotropic fluids. *Arch. Ration. Mech. Anal.* **4** (1), 231–237.

Hall, W.F. & Busenberg, S.N. 1969 Viscosity of magnetic suspensions. *J. Chem. Phys.* **51** (1), 137–144.

Happel, J. & Brenner, H. 1983 *Low Reynolds Number Hydrodynamics*. D. Reidel.

Hinch, E.J. 1972 Note on the symmetries of certain material tensors for a particle in Stokes flow. *J. Fluid Mech.* **54** (3), 423–425.

Hinch, E.J. & Leal, L.G. 1972 The effect of Brownian motion on the rheological properties of a suspension of non-spherical particles. *J. Fluid Mech.* **52** (4), 683–712.

Jiang, S., Schultz, M.J., Chen, Q., Moore, J.S. & Granick, S. 2008 Solvent-free synthesis of Janus colloidal particles. *Langmuir* **24** (18), 10073–10077.

Keh, H.J. & Chen, S.H. 1996 The motion of a slip spherical particle in an arbitrary Stokes flow. *Eur. J. Mech. B/Fluids* **15**, 791–807.

Kim, S. & Karrila, S.J. 1991 *Microhydrodynamics: Principles and Selected Applications*. Butterworth–Heinemann.

Landau, L.D. & Lifshitz, E.M. 1987 *Fluid Mechanics*. Pergamon.

Lighthill, M.J. 1952 On the squirming motion of nearly spherical deformable bodies through liquids at very small Reynolds numbers. *Commun. Pure Appl. Maths* **5** (2), 109–118.

Luo, H. & Pozrikidis, C. 2008 Effect of surface slip on Stokes flow past a spherical particle in infinite fluid and near a plane wall. *J. Engng Maths* **62** (1), 1–21.

Masoud, H. & Stone, H.A. 2019 The reciprocal theorem in fluid dynamics and transport phenomena. *J. Fluid Mech.* **879**, P1.

Nir, A. & Acrivos, A. 1973 On the creeping motion of two arbitrary-sized touching spheres in a linear shear field. *J. Fluid Mech.* **59** (2), 209–223.

Pedley, T.J. 2016 Spherical squirmers: models for swimming micro-organisms. *IMA J. Appl. Maths* **81** (3), 488–521.

Premlata, A.R. & Wei, H.H. 2019 The Basset problem with dynamic slip: slip-induced memory effect and slip–stick transition. *J. Fluid Mech.* **866**, 431–449.

Premlata, A.R. & Wei, H.H. 2021 Coupled Faxen relations for non-uniform slip Janus spheres. *Phys. Fluids* **33** (11), 112003.

Rallison, J.M. 1978 Note on the Faxén relations for a particle in Stokes flow. *J. Fluid Mech.* **88** (3), 529–533.

Ramachandran, A. & Khair, A.S. 2009 The dynamics and rheology of a dilute suspension of hydrodynamically Janus spheres in a linear flow. *J. Fluid Mech.* **633**, 233–269.

Swan, J.W. & Khair, A.S. 2008 On the hydrodynamics of 'slip–stick' spheres. *J. Fluid Mech.* **606**, 115–132.

Wang, S. & Ardekani, A.M. 2012 Unsteady swimming of small organisms. *J. Fluid Mech.* **702**, 286–297.